ADAMA SCIENCE AND TECHNOLOGY UNIVERSITY

SCHOOL OF ELECTRICAL ENGINEERING AND COMPUTING

DEPARTMENT OF ELECTRONICS & COMMUNICATION ENGINEERING

CLASSIFICATION OF UNDER GROUND TARGETS

By

Jima Tulu

A thesis submitted in partial fulfillment of the requirements for the degree of

Master of Science in Communication Engineering

Advisor: Dr. Sultan Feisso

Adama, Ethiopia

March, 2017

Classification of Under Ground Targets

Submitted by:

Jima Tulu ________________ ________________

Student Signature Date

Approved by:

Dr. Sultan Feisso ________________ ________________

Advisor Signature Date

Internal Examiner: ________________ ________________

Dr. M.Venkata Raghuvandra Signature Date

External Examiner: __________________ ________________

Dr. Eristu Yigzaw Signature Date

Chairman, Department: _________________ ________________

Ing. Hinsermu Alemayehu Signature Date

Graduate Committee:

_____________________ _________________ ________________

Signature Date

DECLARATION

I hereby declare that the work which is being presented in the thesis entitled, *classification of underground targets*, submitted to Adama Science and Technology University (ASTU) in partial fulfillment of the requirements for the degree of Master of Science in Communication Engineering, is the result of my own research carried out under the supervision of Dr. Sultan Fiesso and all materials used and reproduced have been properly referred.

Signature: ___________________

Name of candidate: Jima Tulu

Date: _____________________

This is to declare that the above statement made by the candidate is correct and true to the best of my knowledge.

Advisor: Dr. Sultan Fiesso

Signature: ____________________

Date: _____________________

ABSTRACT

Early days of technology to detect landmines employed conventional techniques like Metal detector which is used to measure the disturbance of an emitted electromagnetic field caused by the presence of metallic objects in soil. Recently, GPR has been considered as an appropriate tool for detection of landmine which is used to detect buried objects by emitting radio waves into the ground and then analyzing the return signals generated by reflection of the waves at the boundaries of materials with different indexes of refraction caused by differences in electrical properties.

This study presents an approach to charactering Ground Penetrating Radar (GPR) back scatter signal's echoes from buried land mines using linear combinations of exponentially damped sinusoids. The GPR signatures of landmine PMN2 buried in dry sand soil are measured using stepped frequency radar with frequency of 1.4GHz - 5GHz .The GPR back scattered signal characters are represented as a set of complex poles computed from a reflected signals. Scattering center algorithm proposed by matrix pencil which uses linear prediction along with singular value decomposition is applied to compute the pole.

Keywords: Ground Penetrating Radar, scattering center extraction, Clustering approach, Z plane classification

ACKNOWLEDGMENTS

I would like to thank my advisor, Dr. Sultan Feisso, for giving me the direction, support and knowledge needed in order to perform this research. I would also like to thank all my friends for their support and essential ideas that contributed greatly to my work.

Finally, I would like to thank ORTO and ASTU for believing in my abilities enough to support my graduation education.

Contents

LIST OF FIGURE

List of Tables

LIST OF ACRONYMS

A/D	Analog to Digital
AP	Anti personal
AR	Autoregressive
ARMA	Autoregressive moving average
ATR	Automatic Target Recognition
AWGN	Additive white Gaussian noise
CMP	Common-midpoint measurement
CO	Common off set
CW	Continuous Wave.
dBsm	Decibels relative to one square meter
ED	Euclidean Distance
EM	Electromagnetic Wave
ESPRIT	Estimation of Signal Parameters using Rotational In-variance Time .
GE	Generalized eigen-values
GPOF	Generalized pencil of functions
GPR	Ground penetrating radar
GTD	Geometrical Theory of Diffraction
IDFT	Inverse Discrete Fourier Transform
MA	Moving average
MAUCAZ	Matching Algorithm using Clustering Approach in Z-Plane.
MP	Matrix Pencil
OP	Orthogonal Polarization
PP	Principle Polarization
PRF	Pulse repetition frequency
RCS	Radar Cross Section
RDP	Relative dielectric permittivity
RTI	Radar target identification
SFCW	Stepped frequency continuous wave
SNR	Signal to noise ratio

SVD	Singular Value Decomposition
SVDP	Singular value decomposition prony
TWW	Two Way Travel time wave
UXO	Unexploded ordnance
WARR	Wide-Angle Reflection And Refraction

CHAPTER ONE

INTRODUCTION

1.1. Background

Underground object detection possesses the most challenging problem. The reason being the earth surface consisting of varied kind of materials and all in almost in solid form. The principle of object detection again remain mostly the reflection from varies layers underneath the surface.

Acoustic/seismic methods look for buried object by vibrating them with sound or seismic waves that introduced into the ground. Materials with different properties vibrate differently when exposed to sound waves. These methods are complementary to existing sensors with low false alarm rates and are unaffected by moisture and weather. Existing systems are slow and they do not detect mines at depth, because the resonant response attenuates significantly with depth [1].
Metal detector is used to measure the disturbance of an emitted electromagnetic field caused by the presence of metallic objects in the soil. The popular, basic metal detector is easy and cheap to use and has an average success rate. However, metal detector is limited to detect and identify only metal objects, while the problems to detect other objects remain unsolvable with metal detector.

Biological detection methods involve the use of mammals, insects, or microorganisms to detect explosives. Like chemical sensors, these methods rely on detection of explosive compounds rather than on detection of metal or changes in the physical properties of the subsurface. Thus, they have the potential for reducing false alarm rates from metal clutter. Biological- sensing technology requires an understanding of how explosives migrate away from landmines as well as knowledge of the chemical and physical principles of the sensor [2].
The first use of electromagnetic pulses to determine the structure of buried features appeared in 1926 in the work of Hülsenbeck. He noted that any dielectric variation would also produce reflections and that the technique had advantages over seismic methods. The first ground

penetrating radar survey to be reported was the determination of the depth of a glacier in 1929 by Stern [3] . The systems used in that time were exclusively impulse time domain systems [4]. The applications were mainly found in the domain of civil engineering: location of voids, containers, tunnels and rocks, detection of cables and tubes, measuring the thickness of ice and coal layers, probing the profiles of lakes and rivers, etc. From then until today, the range of applications has been growing steadily.

Ground penetrating radar (GPR) is an emerging technology that provides centimeter resolution to locate even targets that are too small [5]. It is an electromagnetic technique that is designed primarily to investigate roads, Landmine, bridges and subsurface objects. In the last three decades, impulse GPR has been considered as a viable technology for the detection of buried landmines without affecting the environment where the targets are. GPR senses electrical in homogeneities caused by dielectrics of buried objects in the presence of less-conducting ground soil [2]. It is nondestructive geophysical method that produces a continuous cross sectional profile or record of subsurface features, without drilling, probing or digging .GPR profiles are used for evaluating the location and depth of buried objects. Many of the geophysical methods for detection of buried landmines and UXO make use of electromagnetic signals. Among these, ground-penetrating radar (GPR) is considered as a promising technology, because of its ability to detect both metallic and non-metallic AP landmines by non-invasive subsurface sensing. Dielectric medium properties are a critical parameter for this method, because the dielectrics control the contrast between the object of study and the medium it is buried in. Additionally the dielectric medium properties control propagation, attenuation, and reflection of electromagnetic waves. Under some soil conditions the landmine signature is of high quality while under others no signature can be detected at all .Modern landmines are mainly plastic or less metallic that the dielectric contrast between the landmine and the background is very weak. The existence of large contrast between the air and the soil medium causes a strong bounce that returns from the interface which usually obscures the weak signature caused by the buried plastic landmine [6, 7, 8]. The signal reflected from buried plastic landmines is subjected to strong background clutter, noise and distortions. Hence, one of the main challenges of using GPR for landmine detection is to remove the ground bounce as completely as possible without altering the landmine return. Model-based signal processing algorithms for clutter reduction and target discrimination are important in this area. It is expected that a classifier relying on the model-parameters would be less sensitive to these variations. However, taking all the estimated parameters into account may not lead to a robust solution in the light of the results presented earlier. Depending on the accuracy of the model-estimates employed, it is expected that classification performance will vary considerably. The technique proposed here is motivated by three points. First, a more robust classifier could be created by giving a smaller importance to the contribution of the most sensitive model-parameters. Second, it is expected that using reduced but more accurate data provides enough information to achieve better classification. Third, the fact that the set of potential targets is limited intuitively calls for the introduction of a priori information in the modeling process.

Signals are classified by comparing their patterns of poles with templates in a library. A limited number of clusters are formed by associating two poles, one from the test-pattern and the other from the template-pattern, supposedly related to the same physical scatterer on the target. The similarities between two patterns are quantified by means of a mathematical expression that increases with the distance between corresponding poles.

1.2. Objective

1.2.1 General Objective

The main objective of this thesis is to detect and classify buried landmines using supper resolution scattering center extraction algorithm along with Matching Algorithm using Clustering Approach In Z-Plane (MAUCAZ).

1.2.2 Specific Objective

The specific objectives of this thesis will be:

- To measure underground back scattered signals with Ground Penetrating Radar.
- To analysis Scattering center extraction
- To cluster patterns of poles in the z plane
- To analysis MAUCAZ algorithm

.

1.3. Statement of problems

Aircraft flying above a certain altitude are required to be equipped with an electronic transponder whose mission is to report altitude and to provide its identity to civilian or military air traffic control. Although such cooperative systems provide accurate information, one should not rely exclusively on them as serious problems may arise when the transponder is switched off and the targets are buried. Radar appears as a unique sensor that could provide valuable information for achieving automatic target recognition in any conditions. Different techniques are developed which is focused on using powerful processing tools for identifying aircraft based on some kind of a priori knowledge. Radar measurements can provide an image of the reflectivity of a target. Because such signatures depend upon the target structure, an unknown target can be identified by comparing its signature with templates previously generated and stored in a database. But most techniques such as thresholding and correlation matching have been shown to produce high false alarm rate and detect the target with less resolution. Combination of scattering centre extraction algorithm and Matching Algorithm using Clustering Approach Z-plane (MAUCAZ) attempts to find the underlying relationship of input patterns using the assumption that inputs of the same class will be naturally clustered together and classified.

Assuming that the separation of the clutter from the actual target is possible, the joint use of the Scattering centre extraction algorithm and the MAUCAZ algorithm would provide excellent results for buried target.

1.4. Methodology

1.4.1 Theoretical Study

A literature survey was conducted on the area of Ground Penetrating Radar, scattering center extraction and matching algorithm using cluster approach in z-plane for every stage of the system. Available books, journals, case studies, previous research works & guidelines were surveyed in order to have a clear understanding of the subject matter.

1.4.2 Data Collection

The electrical property and reflectivity of soils and subsurface object were collected from Ethiopian Geological agency, Oromia water and construction Bauru and Internet.

1.4.3 Analysis

The radar transmitter produces a short pulse of high frequency electromagnetic energy, which is transmitted into the ground through an antenna. Variations in the electrical impedance within the ground generate reflections that are detected at the ground surface by the same or another antenna attached to a receiver unit. Variations in electrical impedance are largely due to variations in the relative permittivity or dielectric constant of the ground.

First, the backscattered signals were received and pre processed for analysis. Then, the model order selection was performed and pole of signal determined using scattering center extraction algorithm. Finally, the pole feature of test and template signals were extracted and clustered.

Generally, the core thesis work is made up of Ground penetrating radar returned signals data acquisition, extracting the feature of the received signal, clustering the scatterer based on pole similarity and eventually, classifies the buried target

1.5. Significance of the Study

The significance of this study is to classify buried landmines using radar signals based on the target reflectivity pattern properties.

1.6. Scope of the Study

The scope of this thesis is limited to study and classify landmines that are buried in dry sand soil.

1.7. Contribution

So far, a number of researches have been conducted to extract scattering center from Ground Penetrating Radar signals for recognizing landmines and matching algorithm using cluster approach in z-plane to identify and cluster pole patterns of the signals.

Mostly the previous researches focus toward air born targets such as Air craft and Rain drop detection and classification.

Investigating underground objects such as Landmines, water table, natural oil and mines without destructing the environment is becoming very essential and needs more robust technology as that of air born targets.

In addition, the classification must be performed at low cost and efficient way to identify the specific target.

Hence, one of the main challenges of using GPR for landmine detection is to remove the ground bounce noise as completely as possible without altering the landmine return.

Thus, after a thorough literature survey, this work is the first to consider a combination of scattering center extraction algorithm and matching algorithm using cluster approach in z- plane to cluster and classify underground targets, particularly anti-personnel landmines.

Lastly, it incorporates ground penetrating radar to detect and used in demine of metallic and non-metallic landmines without destructing the environment

1.8. Thesis Outline

The remaining parts of thesis are organized as follows: Chapter 2; Literature Review**.** Chapter 3; Ground Penetrating Radar for Detecting Buried Target. Chapter 4; describe Scattering Centre Extraction Algorithm. In Chapter While 5, Matching Algorithm using cluster approach in Z plane In Chapter 6, Design and Implementation

CHAPTER TWO

LITERATURE REVIEW

In this chapter literature review of the detailed processes employed in the thesis work is presented. It includes the Ground Penetrating Radar basics and its principles, Scattering center extraction and matching algorithm using cluster approach in z plane landmine identification and classification technique.

2.1. Correlation-Based Target Classification

2.1.1. Signal-based approach

Herv´e Borrion Described a basic translation-invariant classification technique for achieving alignment and comparison of range profiles using a correlation filter. The system diagram is represented in figure 2.1 [7].

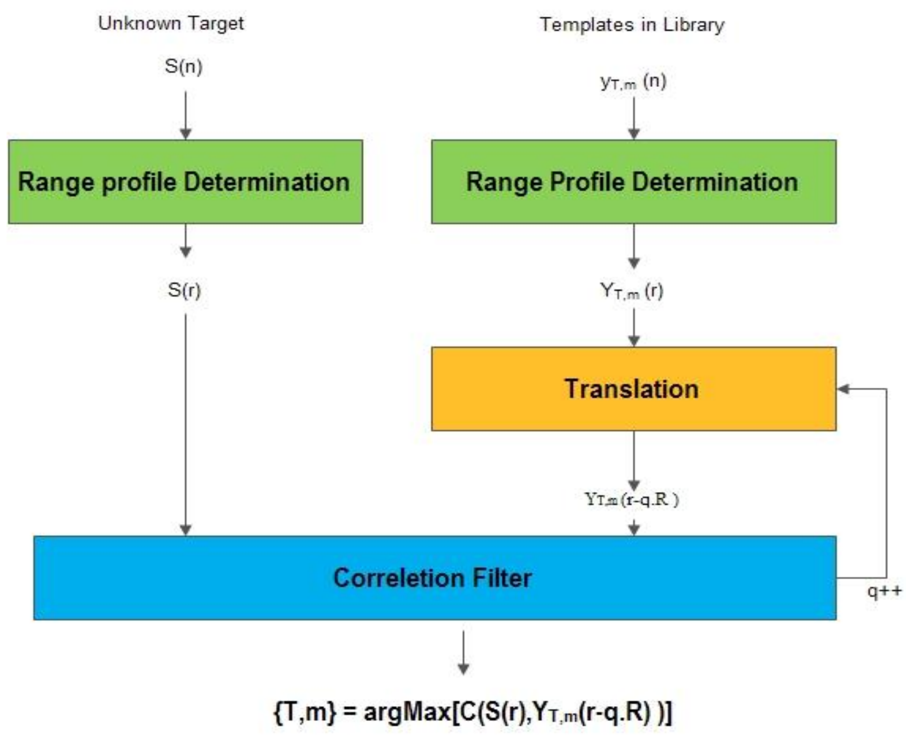

Figure 2.1: Structure of a correlation-based classifier using I/Q radar signals.

The first stages compute the range-profiles, S and $Y_{T,m}$, of the test signals **s** and the templates $y_{T,m}$.

2.1.2. Model-based approach

Model based approach used radar signals, s and y, are replaced by their models, $\hat{s}$ and, $\hat{y}$ in order to benefit from noise removal and resolution enhancement allowed by the super-resolution methods. First, the scattering-centre parameters of the signal in the library, $y_{T,m}$, are computed using the same parameters L and P for both. The corresponding models are reconstructed [8].

Figure 2.2 represents the system diagram of the model-based classification technique. It also relies on cross-correlation of test- profiles and template profiles but uses high-resolution range profiles obtained by determining the scattering-centre models. Here the bandwidth can be artificially enlarged by increasing the number of frequency indices used. Then the same process is applied to the measured signal. Finally, the profiles are aligned and compared by cross-correlation [7].

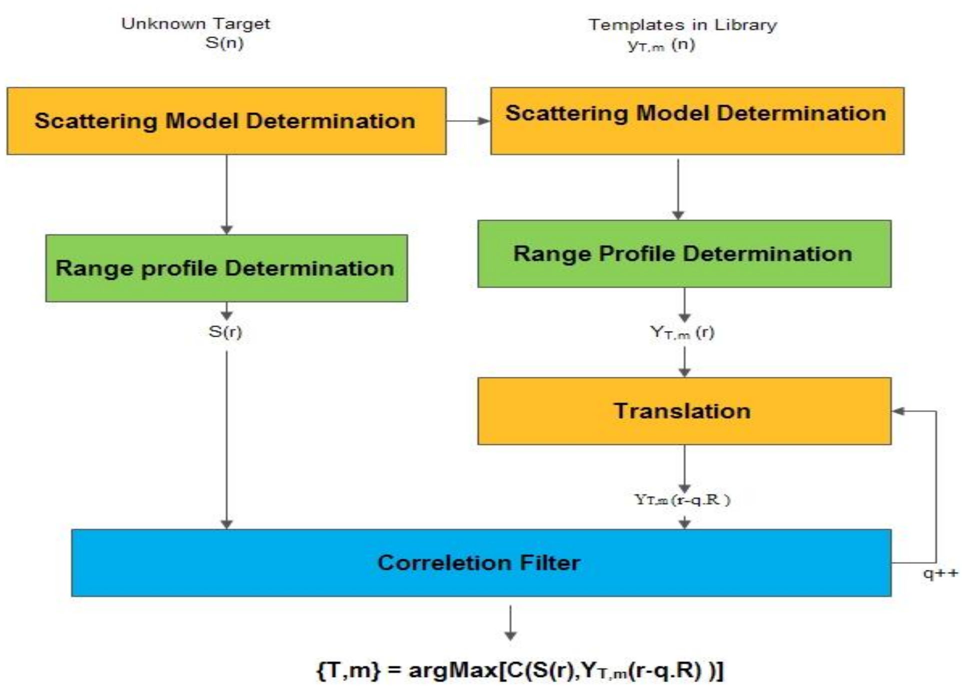

Figure 2.2: Structure of a classifier using scattering-centre models.

Depending on the accuracy of the model, the extrapolation of the original radar signals, s and $y_{T,m}$, is expected to create improved information that results in classification performance enhancement.

2.2. Z-domain classification

Herv´e Borrion introduced classification technique based on the idea that the poles of the model parameters are less sensitive to noise and small variation of aspect-angles than the reconstructed model. It reveals that radar-measurements involving similar targets and similar perspectives should present similarities that can be observed in the pattern of poles expressed in the z-plane. As this is a key requirement for classification, it is believed that a signal could be classified by comparing its pattern of poles with other pole template-patterns in library. Physically each measurement is classified based on the probability that the target shares a common arrangement of scatterers in range with other targets in library [7].

In general the Z-domain classification of targets based on the pattern of poles includes the conventional stages including pre-processing, feature-selection, and classification. Several issues that are specific to this comparative approach are addressed in this chapter. They include the way to measure the similarity between patterns of poles, the features to use for the comparison, the differentiation between true poles and extraneous poles, whether the latter are due to the noise, to the technique, or even to extra scatterers on the target. Finally, the problem of alignment, which is common to most classifiers is taken into account.

Z-plane classification is achieved by comparing radar-signals based on features that are visible in the pattern of poles in the z-plane; the latter being related to the scattering function. In the pre-processing stage, data are prepared for feature-selection. Figure 2.3 represents the system diagram leading to the determination and selection of the poles using both the test-signal and the templates in library.

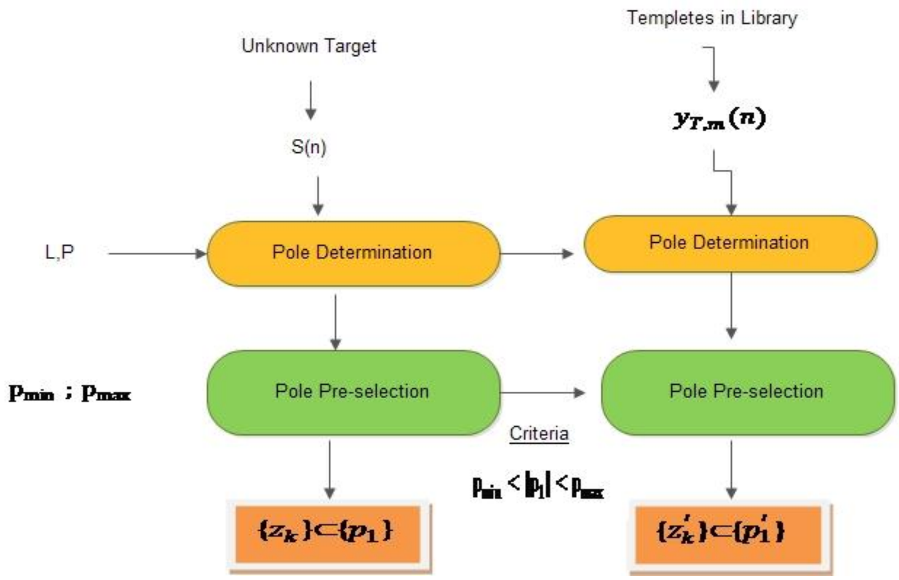

Figure 2.3: MAUCAZ system diagram - pre-processing stage

Signals are classified by comparing their patterns of poles with templates in a library. A limited number of clusters are formed by associating two poles, one from the test-pattern and the other from the template-pattern, supposedly related to the same physical scatterer on the target. The similarities between two patterns are quantified by means of a mathematical expression that increases with the distance between corresponding poles. This method enables the classifier to take into account the variations of the poles mentioned above.

This cost-function is calculated for each pattern in the library, that is, for measurements involving various types of aircraft and various aspect-angles. Assuming that the minimal distance corresponds to the maximum similarly, it is expected that the best match corresponds to the minimum value of the cost function.

2.3. Landmine Detecting Techniques

Low and non-metallic landmines are one of the most difficult subsurface targets to be detected using several geophysical techniques. Ground penetrating radar (GPR) performance at different field sites shows great success in detecting metallic landmines. However significant limitations are taking place in the case of low and non-metallic landmines. Electrical resistivity imaging (ERI) technique is tested to be an alternative or confirmation technique for detecting the metallic and non-metallic landmines in suspicious cleared areas. The electrical resistivity responses using forward modeling for metallic and non-metallic landmines buried in dry and wet environments utilizing the common electrode configurations have been achieved. Roughly all the utilized electrode arrays can establish the buried metallic and plastic mines correctly in dry and wet soil. The accuracy differs from one array to the other based on the relative resistivity contrast to the host soil and the subsurface distribution of current and potential lines as well as the amplitude of the noises in the data. The ERI technique proved to be fast and effective tool for detecting the non-metallic mines especially in the conductive environment whereas the performances of the other metal detector (MD) and GPR techniques show great limitation [10].

The current conventional deminer tools include in principle metal detector (MD), mechanical prods (like steel prod or screw diver) and sometimes well trained doges (MacDonald et al., 2003). However, the MD technique does not entirely detect low and non-metallic landmines moreover the limitation is significant in the highly ferruginous soil environment (Lopera and Milisavljevic, 2007). Recently, there are a number of noninvasive geophysical techniques have been included in the landmine detections. Among these techniques is the ground penetrating radar (GPR) which is potentially promising in locating metallic, low and non-metallic mines at different host soil (MacDonald et al., 2003). The success of GPR performance is remarkably whereas there is a considerable contrast in dielectric properties between the landmine

The detection of land mines has been a very important and popular research area in recent years. Nowadays the unstable world also highlights the importance of land mine detection technique. Widely published reports estimate that there are 110 million land mines in 70 countries [11].
The land mine detection is a problem of significant military, economic, and humanitarian concern. Not only do land mines pose a deterrent to military activity during conflict, they also remain lethal long after that conflict is over . So the research is driven not only by the need in military operations, but also for humanitarian purposes to clear up mine fields left after wars that claim more than 30,000 deaths and injuries every year . The statistics are staggering: 80 percent of the victims of antipersonnel mines are civilians, many of whom are children . Moreover, the

number of anti-personnel land mines is increasing at the rate of one half to one million mines per year [11].

Ground-penetrating radar (GPR) is a sensor which has a good potential for use in buried land mine detection. Compared to metal detectors (EMI sensors), GPR can detect both metallic and non-metallic objects, and has the capability of imaging the target shape. However, application of GPR to mine detection has suffered from many technical problems. The dielectric properties of objects are essential in GPR surveying, and in practical situations, soil moisture and soil inhomogeneity are the most important parameters to consider in mine detection by GPR [12].

[Xavier Núñez-Nieto] Described Ground penetrating radar (GPR), which has proven to be suitable for subsoil investigations, is a technique that has been recognized by the scientific community for mine and UXOs detection . GPR has been proposed as a solution for mine clearance and the removal of unexploded ordnance because of its speed, safety and suitability as a non-invasive technique compared to more invasive methods that are commonly used in demining operations, such as excavations or traditional detection methods, such as metal detectors, which may be dangerous. GPR has significant advantages over the standard electromagnetic induction (EMI) technique, because it allows improved discrimination of small metal fragments . Military organizations, universities and private companies have developed specific research programs, such as the International Advanced Robotics Programme (IARP), that are based on the design of vehicles that are focused exclusively on the problem of humanitarian demining [13].

2.4. Matrix Pencil

Yingbo Hua described a study of a matrix pencil method for estimating parameters (frequencies and damping factors) of exponentially damped and/or undamped sinusoids in noise. Comparison of this method to a polynomial method (SVD-Prony method) shows that the matrix pencil method and the polynomial method are two special cases of a matrix prediction approach but the pencil method is more efficient in computation and less restrictive about signal poles. It is found through perturbation analysis and simulation that, for signals with unknown damping factors, the pencil method is less sensitive to noise than the polynomial method [14].

2.5. Signal Resolution

The successful detection of underground objects or structures is primarily restricted by the resolution of the measurement. This is the ability to distinguish two nearby structures or signals which are temporally close to each other. For the spatial resolution the wavelength $\boldsymbol{\lambda}$ of the electromagnetic signal is relevant. Are two reflectors separated by more than half a wavelength ($\frac{\lambda}{2}$) they are usually well distinguishable in a radar-gram. Under very good conditions, the signal resolution can reduce to about one fourth of wavelength ($\frac{\lambda}{4}$). From the relationship of the propagation velocity **v** with the wavelength $\boldsymbol{\lambda}$ and the frequency f: $\boldsymbol{\lambda} = \frac{v}{f}$ it is obvious that the smaller the wavelength and the higher the frequency, the higher is also the spatial resolution of the measurement [21].

2.6. Scattering Center Extraction

In the high-frequency region where most radar systems operate, it is often assumed that man-made targets can be accurately represented by a set of isolated scattering points. These scatterers generally correspond to discontinuities on the target. For instance, the main scattering centers on an aircraft are the radome, the leading edge of a wing or an engine duct. It follows that the radar return from a target can be described as the result of individual contributions from many sources. This has been introduced by Keller under the name of Geometrical Theory of Diffraction (GTD) [22].

Given N measurements at frequency $f_n = f_0 + n.\Delta f$ the scattering centre model for the electric field backscattered is given by ŝ(n) [23].

$$\acute{s}(n) = \sum_{k=1}^{M} a_k.\left(\rho e^{-j\phi_k}\right)^n$$

Where M is the number of scatterers in the model, a_k is the complex-valued amplitude term associated with the reflectivity of the k^{th} target, ρ^k is the real-valued frequency dependent amplitude and ϕ_k is the phase angle related to the time-delay. In radar, the backscattered signal is generally written as a deterministic signal s(n) corrupted by an additive white Gaussian noise (AWGN) u(n):

$$x(n) = s(n) + u(n)$$

The approach is to find a model ŝ(n) that matches the signal x(n). The set of parameters {a,ρ,ϕ}k are determined from the complex-valued reflectivity samples in the frequency domain. In observation science, physical mechanisms are often described as linear mechanisms for simplicity. In this case, we assume that one frequency sample is related to the L previous samples by an autoregressive (AR) model [24].

$$\sum_{l=0}^{L-1} x(L+m).g(l) = x(L+m)$$

Where g(l) are the autoregressive coefficients and m is the row-index. Following equation (3), the N samples x(n) are organized in an observation matrix HR×L known as the backward-data matrix by opposition to the forward-data matrix. The special form of this Toeplitz matrix H is called the Hankel matrix [25].

$$H = \begin{bmatrix} x(0) & x(1) & x(2) & \dots & x(L-1) \\ x(1) & x(2) & x(3) & \dots & x(L) \\ x(2) & x(3) & x(4) & \dots & \vdots \\ \vdots & \vdots & \ddots & \ddots & \vdots \\ x(R-1) & x(R) & \dots & \dots & x(N) \end{bmatrix} \quad (2.12)$$

Assuming that the noiseless data sequence s(n) is composed of undamped complex exponentials (ρk=1), any row of H can be written as a linear combination of the following M linearly independent vectors:

2.7. Matching Algorithm

2.7.1. Understanding Cluster Analysis

Cluster analysis groups objects (observations, events) based on the information found in the data describing the objects or their relationships [26]. The goal is that the objects in a group should be similar (or related) to one another and different from (or unrelated to) the objects in other groups. The greater the similarity (or homogeneity) within a group and the greater the difference between groups, the better the clustering [27].

Cluster analysis divides data into meaningful or useful groups (clusters). If meaningful clusters are the goal, then the resulting clusters should capture the "natural" structure of the data. For example, cluster analysis has been used to group related documents for browsing, to find genes and proteins that have similar functionality, and to provide a grouping of spatial locations prone to earthquakes [28]. However, in other cases, cluster analysis is only a useful starting point for other purposes, e.g., data compression or efficiently finding the nearest neighbors of points. Whether for understanding or utility, cluster analysis has long been used in a wide variety of fields: psychology and other social sciences, biology, statistics, pattern recognition, information retrieval, machine learning, and data mining [28].

In this chapter we provide a short introduction to cluster analysis, and then focus on the challenge of clustering high dimensional data. We present a brief overview of several recent techniques, including a more detailed description of recent work of our own which uses a concept-based approach. In all cases, the approaches to clustering high dimensional data must deal with the "curse of dimensionality", which, in general terms, is the widely observed phenomenon that data analysis techniques (including clustering), which work well at lower dimensions, often perform poorly as the dimensionality of the analyzed data increases.

CHAPTER THREE

GROUND PENETRATING RADAR FOR DETECTING BURIED TARGET

3.1 Introduction

This research depends on data provided by GPR for underground target characterization and its recognition of objects. Hence, this chapter of the report deals with the working principle of GPR ,Radar cross section (RCS) and its processing to extract the features of underground buried objects for classification. The necessary back scattered signal modeling processing techniques required before classification are all addressed.

3.2 Ground Penetrating Radar Basic Principles

Ground Penetrating Radar (GPR) is a geophysical method that uses EM wave designed primarily to locate an object that are buried beneath the earth's surface. A GPR system uses the difference in the permittivity of both the target and the surrounding medium to detect a target. A target is declared present if the GPR detect a local change (or discontinuity) in the media's (such as soil) dielectric [6]. Electromagnetic wave is radiated from Ground penetrating Radar's transmitting antenna, travels through the material at a velocity which is determined primarily by the relative permittivity, relative permeability and conductivity of the material. The wave spreads out and travels downward until it hits an object that has different electrical properties from the surrounding medium, is scattered from the object, and is detected by a receiving antenna. The surface surrounding the advancing wave is called a wave-front. A straight line drawn from the transmitter to the edge of the wave front is called a ray. Rays are used to show the direction of travel of the wave front in any direction away from the transmitting antenna. If the wave hits a buried object, then part of the wave's energy is "reflected" back to the surface, while part of its energy continues to travel downward. The wave that is reflected back to the surface is captured by a receive antenna, and recorded on a digital storage device for later interpretation.

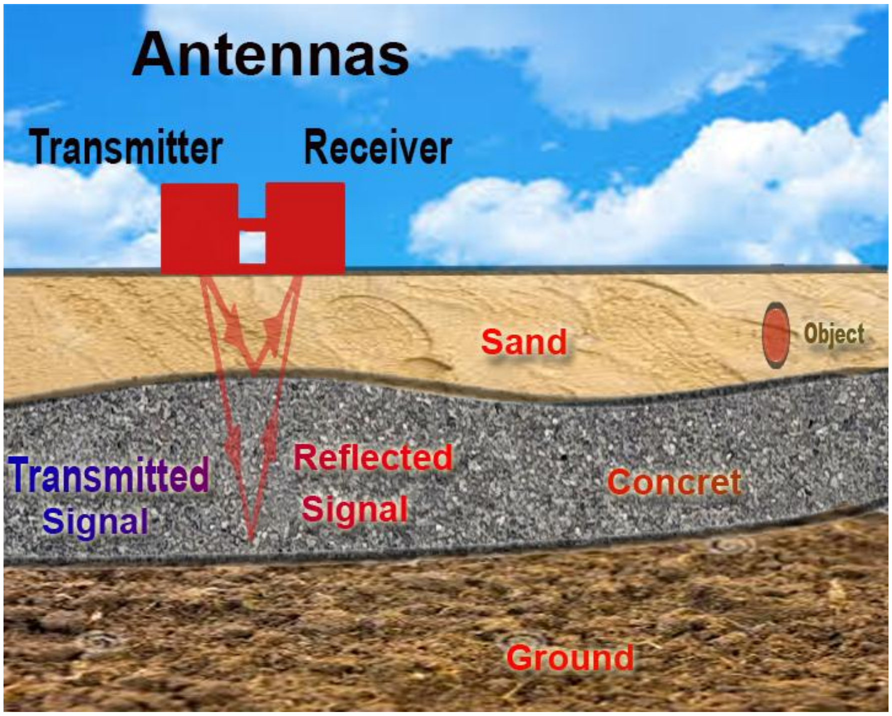

Figure 3. 1.Basic functional principle of a GPR device.

In genera the EM wave is reflected at positions where the penetrated material changes which caused by a change of the EM properties in the subsurface; the permittivity (ε), the permeability (μ) and electrical conductivity (δ). However, not all three parameters provide useful information to the GPR. Conductivity generally affects the penetration depth of the GPR due to absorption of the radar signals in the medium. Soil with high moisture content increases the electrical conductivity, thus decreasing penetration.

Electromagnetic waves travel at a specific velocity that is determined primarily by the permittivity of the material. The relationship between the velocity of the wave and material properties is the fundamental basis for using GPR to investigate the subsurface. To state this fundamental physical principle in a different way: the velocity is different between materials with different electrical properties, and a signal passed through two materials with different electrical properties over the same distance will arrive at different times. The interval of time that it takes for the wave to travel from the transmit antenna to the receive antenna is simply called the travel time.

When the transmitted EM wave encounter changes in subsurface materials, the properties of the wave are altered, and part of the wave is reflected back to the surface, where data on its amplitude, wavelength, and two-way travel time are collected for analysis and interpreted accordingly. The amplitude and phase of the “echoes” can give information about the scattering properties of the target whilst the time of arrival of different pulses gives indirect distance indications to the subsurface layers of reflectors.

3.3 Data Collection Parameters

There are numerous parameters that can be varied and controlled to achieve the targeted depth and resolution during a GPR survey. These parameters are described in the following section:

3.3.1 Velocity (v)

Velocity (v) of an electromagnetic wave is a function of its frequency (f), the speed of light in free space, and the host medium’s relative dielectric permittivity (ε_r), relative magnetic permeability (μ_r) and conductivity (σ). Mathematically it is defined as:

$$V= \frac{C_o}{\sqrt{\mu_r \varepsilon_r \frac{1+\sqrt{1+\left(\frac{\sigma}{\omega\varepsilon}\right)^2}}{2}}} \qquad (3.1)$$

Where C_o is the electromagnetic wave velocity in a vacuum ($3x10^8 \frac{m}{s}$), and $\frac{\sigma}{\omega\varepsilon}$ is a loss factor, where $\omega = 2\pi f$ is angular frequency (rad/s).For low-loss materials, such as clean sand and gravel, the influence of σ over the GPR frequency range is minimal and it is assumed that $\frac{\sigma}{\omega\varepsilon} \approx 0$. As little is known about magnetic response at radar frequencies, the influence of μ_r is also assumed to be negligible, and is given a value corresponding to nonmagnetic material (μ_r= 1). As a result, Eq. (3.1) can be simplified to:

$$V= \frac{C_o}{\sqrt{\varepsilon_r}} \qquad (3.2)$$

3.3.2 Amplitude

As the electromagnetic wave propagates through a medium, its amplitude (A) shows an exponential decline from its initial value (A_o) as it travels distance z, as follows:

$$A = A_o e^{-\alpha z} \quad (3.3)$$

Where:

α is the attenuation constant. For low-loss materials this constant is frequency independent, such that:

$$\alpha = \frac{\sigma}{2}\sqrt{\frac{\mu}{\varepsilon}} \quad (3.4)$$

It can be seen from Eq. (3.4) that conductivity exerts the greatest influence over the attenuation constant.

3.3.3 Depth of penetration

It has already been demonstrated that propagating electromagnetic waves undergo energy losses in the subsurface. These limit the depth that radar waves can penetrate at a particular frequency or location. The frequency-dependent nature of attenuation means that, in general, the higher the antenna's frequency, the shallower the depth of penetration

The depth to an observed interface can be calculated from this formula (for monostatic antennas):

$$S = V.t = \frac{0.5 x twt x c}{\sqrt{\varepsilon_r}} \quad (3.5)$$

Where:

twt = two way travel time wave.

3.3.4 Wavelength

Wavelength can be described as a propagating wave which repeats itself at a particular distance and is measured in meters:

$$\lambda = \frac{v}{f} \tag{3.6}$$

GPR antennas can typically be distinguished when moving over buried objects features aligned perpendicular to the direction of travel if they are spaced at least one half of a wavelength apart ($\frac{\lambda}{2}$.) Features that are stacked on top of each other can typically be distinguished if they are at least a quarter of a wavelength apart ($\frac{\lambda}{4}$.) [49]. However, features that are closer to each other than these distances may appear as a single feature in GPR data.

3.3.5 Reflection Coefficient

The amount of energy reflected, with respect to signal amplitude, is given by the reflection coefficient (R). Assuming that σ and μ_r contrasts are negligible:

$$R = \frac{\sqrt{\varepsilon_{r2}}-\sqrt{\varepsilon_{r1}}}{\sqrt{\varepsilon_{r2}}+\sqrt{\varepsilon_{r1}}} \tag{3.7}$$

Where ε_{r2} and ε_{r1} are the relative dielectric permittivity of adjacent layers 1 and 2, or:

3.3.6 Transmission Coefficient

The amount of energy transmitted, with respect to signal amplitude, is given by the transmission coefficient (T). Assuming that σ and μ_r contrasts are negligible:

$$T = \frac{2\sqrt{\varepsilon_{r2}}}{\sqrt{\varepsilon_{r2}}+\sqrt{\varepsilon_{r1}}} \tag{3.8}$$

or

$$T = \frac{2\sqrt{V_2}}{\sqrt{V_2}+\sqrt{V_1}} \qquad (3.9)$$

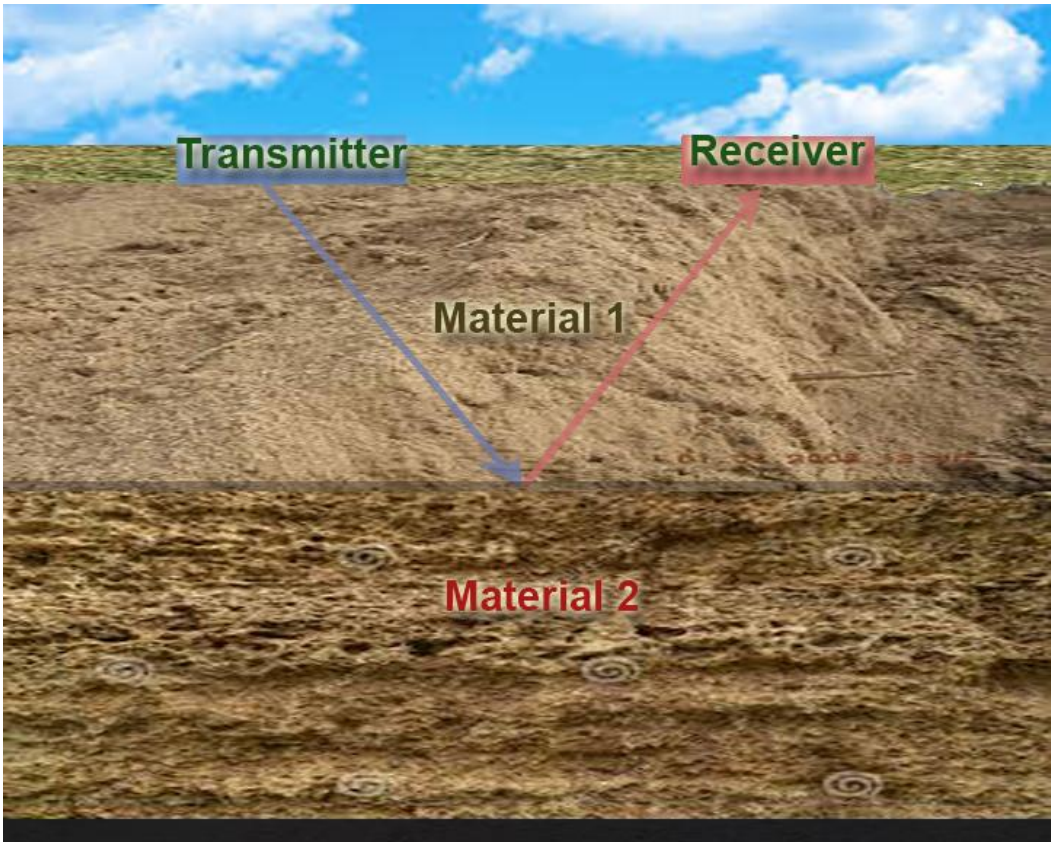

Figure 3. 2. Outline arrangement of GPR system

3.4 Radar Data Acquisition Modes

There are four main modes of radar data acquisition. Following we define these modes.

3.4.1 Common offset

In Common offset mode operation, the transmitter and receiver antennae are at a fixed distance and moved over the surface simultaneously. The measured travel times to radar reflectors are displayed on the vertical axis, while the distance the antenna has travelled is displayed along the horizontal axis in a radar gram display. Most GPR surveys use a common offset survey mode. This mode of data acquisition can be used to improve the azimuth or plan resolution, where a long aperture is synthesized along the azimuth line. Figure 3.3 shows a common offset bistatic mode data acquisition configuration.

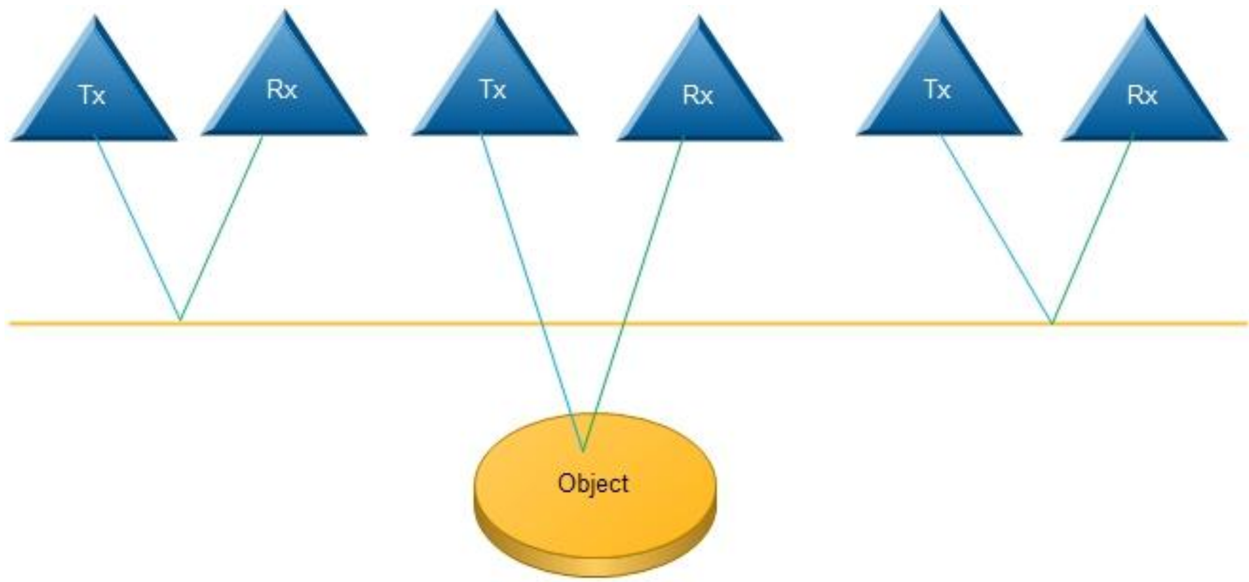

Figure 3. 3. Common offset bi-static mode data acquisition configuration

3.4.2 Common Source Point

In a common source data acquisition system, sometimes called wide-angle reflection and refraction (WARR) sounding [28], the transmitter is kept at a fixed location and the receiver is moved away at increasing offsets. This type of data acquisition mode is most suitable in an area where the material properties are uniform and the reflectors are planar in nature. Figure 3.4 shows the antennae configuration of a common source data acquisition mode.

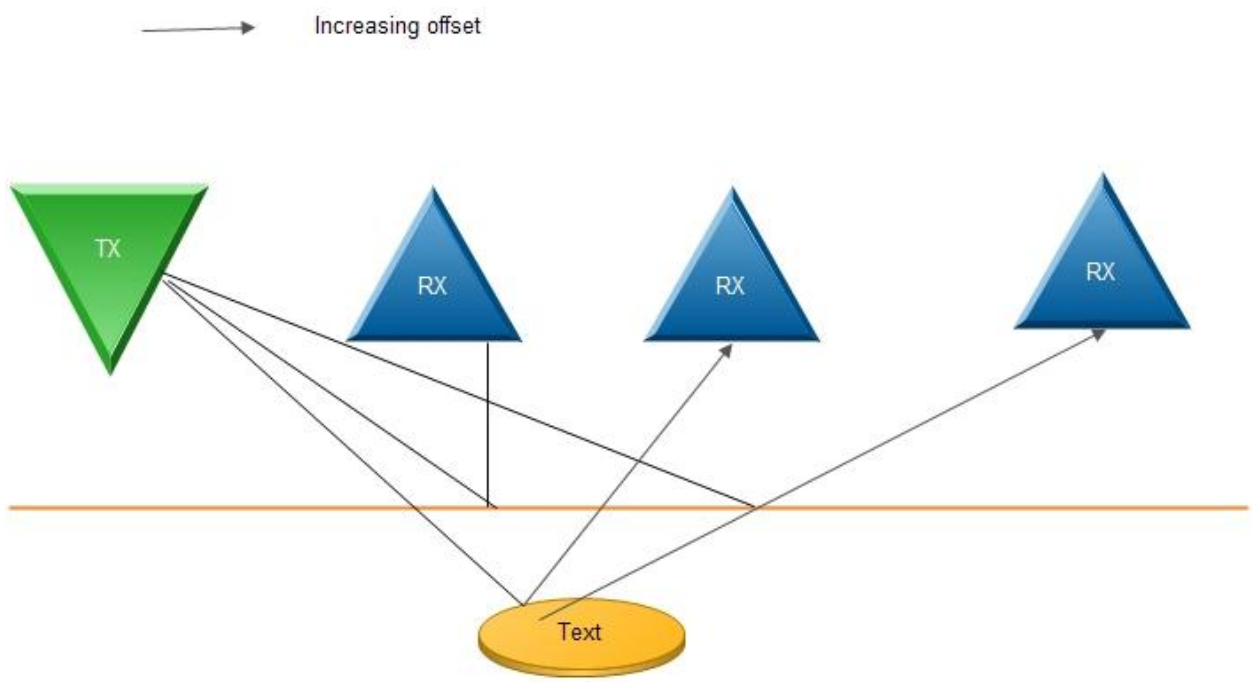

Figure 3. 4. Common source antenna configuration

3.4.3 Common Receiver Point

In common receiver point the data were acquired at the same receiver point for different source points. Figure 3.5 shows the configuration of a common source data acquisition mode.

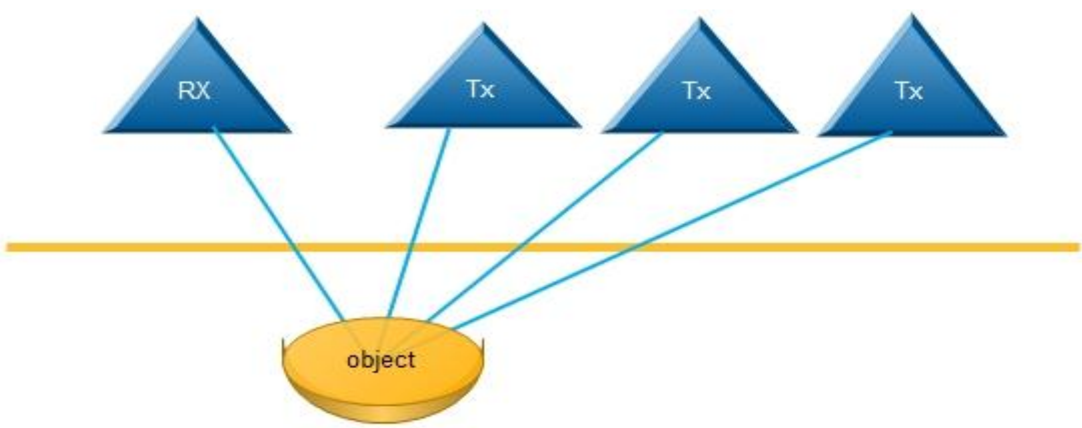

Figure 3. 5. Common receiver antenna configuration

3.4.4 Common Midpoint

In this type of acquisition mode, the transmitter and receiver antennae are moved away at increasing offsets so that the midpoint between them stays at a fixed location. In this case, the point of reflection on each sub-surface reflector is used at each offset, and thus a real consistency at depth is not a requirement. Figure 3.6 shows the antenna configuration of the common midpoint data acquisition mode.

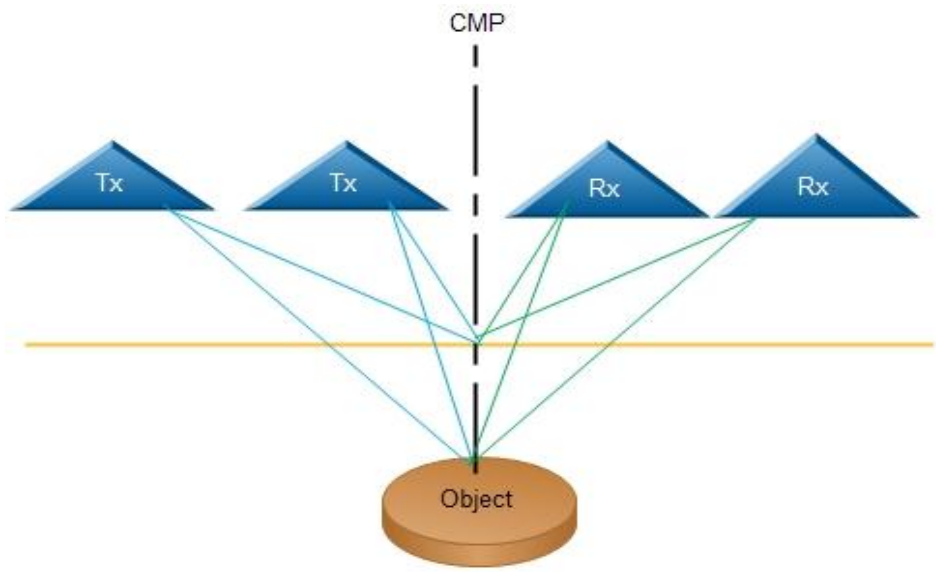

Figure 3. 6. Common midpoint (CMP) measurement configuration

3.5 Radar Cross Section (Rcs)

Radar cross section is the measure of how detectable an object is with a **radar or** a target's ability to reflect radar signals in the direction of the radar receiver, i.e. it is a measure of the ratio of backscatter power per steradian (unit solid angle) in the direction of the radar (from the target) to the power density that is intercepted by the target. A larger RCS indicates that an object is more easily detected.

The RCS of a target can be viewed as a comparison of the strength of the reflected signal from a target to the reflected signal from a perfectly smooth sphere of cross sectional area of 1 m^2.

The conceptual definition of RCS includes the fact that not all of the radiated energy falls on the target. A target's RCS (F) is most easily visualized as the product of three factors:

RCS (F) = **Projected cross section** x **Reflectivity** x **Directivity.**

RCS (F) is used for representing power reradiated from the target.

Reflectivity: The percent of intercepted power reradiated (scattered) by the target.

Directivity: The ratio of the power scattered back in the radar's direction to the power that would have been backscattered had the scattering been uniform in all directions (i.e. isotropically).

Electromagnetic waves, with any specified polarization, are normally diffracted or scattered in all directions when incident on a target. These scattered waves are broken down into two parts. The first part is made of waves that have the same polarization as the receiving antenna. The other portion of the scattered waves will have a different polarization to which the receiving Antenna does not respond. The two polarizations are orthogonal and are referred to as the Principle Polarization (PP) and Orthogonal Polarization (OP), respectively. The intensity of the backscattered energy that has the same polarization as the radar's receiving antenna is used to define the target RCS. When a target is illuminated by RF energy, it acts like an antenna, and will have near and far fields. Waves reflected and measured in the near field are, in general, spherical. Alternatively, in the far field the wave fronts are decomposed into a linear combination of plane waves.

Assume the power density of a wave incident on a target located at range **R** away from the radar is $\boldsymbol{P_{Di}}$. The amount of reflected power from the target is :

$$P_r = \sigma P_{Di} \qquad (3.10)$$

Where:

$,\sigma$ denotes the target cross section.

Define P_{Dr} as the power density of the scattered waves at the receiving antenna. It follows that

$$P_{Dr} = \frac{P_r}{4\pi R^2} \qquad 3.11$$

Equating Eqs. (3.10) and (3.11) yields

$$\sigma = 4\pi R^2 \left(\frac{P_{Dr}}{P_{Di}}\right) \qquad (3.12)$$

and in order to ensure that the radar receiving antenna is in the far field (i.e., scattered waves received by the antenna are planar), Eq. (3.12) is modified.

$$\sigma = 4\pi R^2 \lim_{R\to\infty} \left(\frac{P_{Dr}}{P_{Di}}\right) \qquad 3.13$$

The RCS defined by Eq. (3.13) is often referred to as either the mono-static RCS, the backscattered RCS, or simply target RCS.

The backscattered RCS is measured from all waves scattered in the direction of the radar and has the same polarization as the receiving antenna. It represents a portion of the total scattered target RCS σ_t, where $\sigma_t > \sigma$. Assuming spherical coordinate system defined by (ρ, θ, φ), then at range ρ the target scattered cross section is a function of (θ, φ). Let the angles (θ_i, φ_i) define the direction of propagation of the incident waves. Also, let the angles (θ_s, φ_s) define the direction of propagation of the scattered waves. The special case, when $\theta_i = \theta_s$ and $\varphi_i = \varphi_s$, defines the mono-static RCS. The RCS measured by the radar at angles $\theta_s \neq \theta_i$ and $\varphi_s \neq \varphi_i$ is called the bi-static RCS.

The total target scattered RCS is given by:

$$\sigma_t = \frac{1}{4\pi} \int_{\varphi_s=0}^{2\pi} \int_{\theta_s=0}^{\pi} \sigma(\theta_s, \varphi_s) \sin\theta_s \, d\theta d\varphi_s \qquad 3.14$$

The amount of backscattered waves from a target is proportional to the ratio of the target extent (size) to the wavelength, λ , of the incident waves. In fact, radar will not be able to detect targets much smaller than its operating wavelength. For example, if weather radars use L-band frequency, rain drops become nearly invisible to the radar since they are much smaller than the wavelength. RCS measurements in the frequency region, where the target extent and the wavelength are comparable, are referred to as the Rayleigh region. Alternatively, the frequency region where the target extent is much larger than the radar operating wavelength is referred to as the optical region. In practice, the majority of radar applications falls within the optical region.

As the name suggests, the RCS has dimensions of area: metre-squared. In general, it is given in decibels relative to one square metre (dBsm) because it may vary over rather wide limits. The RCS in m^2 can be converted into dBsm by the following equation.

$$\sigma(dBsm) = 10\log_{10}\left(\frac{\sigma}{1m^2}\right) \qquad (3.15)$$

Some values for RCS

The following table provides typical values of RCS for the frontal sector of different types of target [52].

Table3. 1. RCS for frontal sector of common materials

RN	Type	RCS in m^2	RCS in dBsm
1	Large Commercial plane	100	20
2	Larger fighter	5	7
3	Smaller fighter	2.5	4
4	Man	1	0
5	F-17 fighter	0.03	-15
6	Small Bird	0.01	-20

For simple targets, the frequency dependence of canonical scattering geometries is given by the following table [37].

Table3. 2. Frequency dependency of canonical scattering geometries

RN	Surface Type	Example	α
1	Corner Reflector	Dihedral,Plate	1
2	Singly Curved	Cylinder	0.5
3	Double Curved, Straight Edge	Spheroid	0
4	Curved edge	Circular disk	-0.5
5	Vertex	Cone tip	-1

3.6 Modeling the Signals

The idea of signal modeling is to represent the signal via some model parameters. Signal modeling is used for signal compression, prediction, reconstruction and understanding. In signal analysis, the signals to be detected usually contain unknown parameters such as amplitude, time delay, phase, and frequency; these parameters must be estimated prior to the signal detection. The techniques used to estimate these signal parameters can be broadly classified into two main categories known as parametric and non-parametric methods.

3.6.1 Parametric and non-parametric signal parameter estimation techniques

Non-parametric techniques are Fourier-based methods of providing spectral estimates where no prior model is assumed, in the sense that no assumptions are made concerning the physical process that generated a given data. They are also known as the classical methods of spectral estimation. Although this approach of signal parameter estimation is computationally efficient,

it however has limited frequency resolution. These methods also suffer from spectral leakage effects that often mask weak signals. Prominent conclusions from these non-parametric techniques are that there is always a compromise in the bias variance trade-off because both of these errors cannot be minimized simultaneously [2-5].

Parametric-based methods can however be used to extract high-resolution estimates, especially in applications where short data records are available due to transient phenomena, provided the signal structure is known. These techniques are also known as model-based methods of spectral estimation, where a generating model with known functional form is assumed. The parameters in the assumed model are then estimated, and a signal's spectral characteristics of interest derived from the estimated model. Therefore, the estimated spectral characteristics are only as good as the underlying model. Examples of these parametric-based techniques include the autoregressive (AR) process model [4, 6] and least squares methods [4]), the moving average (MA) process model, as well as the combined autoregressive moving average (ARMA) process model [2-4]. The autoregressive process model, such as the Prony algorithm, is the simplest of the parametric-based techniques. The Prony algorithm, which models sampled data as a linear combination of exponentials, is a technique that can be used for identifying the frequencies, amplitudes, and phases of a signal. Although the Prony algorithm has the ability to resolve rays much closer than the Fourier-based limit, it however has a tendency to yield biased estimates. An improved version of the Prony algorithm, named “singular value decomposition followed by prony-type root recovery,” is often referred to as singular value decomposition prony (SVDP).

For a target consisting of m scatterers is illuminated using a CW radar, then the backscattered field received by a Radar receiver antenna will give a signal of the form:

$$y_k = \sum_{i=0}^{m} A_i e^{\frac{-j2r_i 2\pi f_k}{c}} (j2\pi f_k)^{t_i} \tag{3.16}$$

where

A_i is the amplitude of signal

r_i the relative range of target

t_i the type of the i^{th} scatterer

f_k is the k^{th} frequency

m is the number of scatterers

for stepped frequencies simple we can represent f_k by:

$$f_k = f_0 + k\delta_k \,;\, k = 0,1,2,\ldots,N-1 \tag{3.17}$$

Where:

f_0, δ_k and N are given parameters of the system under consideration.

f_0 represents the lowest frequency the radar system transmits

δ_k is the size of the frequency step

N measurements

By approximating a factor $(j2\pi f_k)^{t_i}$ by a factor of the form p_i^k for some ρ_i .we can model our data as below:

$$y_k = \sum_{i=1}^{m} d_i p_i^k \tag{3.18}$$

where d_i is in general not equal to K_i in (3.16) because of the approximation involved. The variable p_i can be found from:

$$p_i = \rho_i e^{\frac{-j2r_i 2\pi f_k}{c}} \tag{3.19}$$

or, conversely, we can find ρ_i and r_i from p_i by:

$$\rho_i = |p_i| \qquad 3.20)$$

$$r_i = \left(\frac{1}{2} - \frac{\arg p_i}{2\pi}\right)R \tag{3.21}$$

The amount of energy associated with a scattering center can found by considering the contribution of a single scattering center to the total signal. The single scattering center component is: $\{d_i p_i^k\}_{k=0}^{N-1}$

The energy is the square of the absolute value of this contribution, or

$$p_i = \sum_{k=0}^{N-1} |d_i|^2 |p_i|^{2k} \approx |d_i|^2 \frac{1-\rho_i^{2N}}{1-\rho_i^2} \tag{3.22}$$

3.7 Use of the Singular Value Decomposition

Estimation of parameters from a short data record is a difficult problem; while most popular techniques are quite good at estimating parameters from noisy data if the record length is large, their ability to perform well for short records is significantly less. One technique modern signal processing research has found to combat this effect is the use of the Singular Value Decomposition (SVD). The SVD is an orthogonal decomposition technique for matrices; it can be regarded as a generalization of the eigen value decompositions that exist for square matrices.

The use of the SVD to the estimation problem lies in its ability to help determine the rank of a noisy matrix. Recall that estimating the polynomial A(z) requires forming a matrix out of the noisy data . In the noiseless case, the rank of this matrix is m, the number of scattering centers on the target. However, due to the effect of the noise on the data, the actual rank will be greater than m. For small noise variances, the data matrix will be "close" to a matrix of rank m, and the SVD can help find the closest rank m approximation. It is expected that this will reduce the effects of the noise on the estimate (7,8,9].

Next we need to consider how to implement the SVD technique in our algorithm. To do this we modify equation (3.2) as follows: we first compute the matrix on the left of (3.2) and then compute its SVD:

$$Y = U\Sigma V^H \qquad (3.23)$$

where Y is the data matrix, U and V are unitary matrices, and Σ is a diagonal matrix, given by:

$$\Sigma = \begin{bmatrix} \sigma_1 & 0 & \dots & 0 \\ 0 & \sigma_2 & \cdots & 0 \\ \vdots & \vdots & \vdots & \vdots \\ 0 & 0 & \vdots & \sigma_{M+1} \\ 0 & 0 & & 0 \\ \vdots & \vdots & \dots\dots & \vdots \\ 0 & 0 & \dots & 0 \end{bmatrix}_{(N-M-1)x(M+1)} \qquad (3.24)$$

$$\text{Where} \quad \sigma_1 \geq \sigma_2 \geq \cdots \geq \sigma_{M+1} \geq 0 \qquad (3.25)$$

As noted above, if the SNR is sufficiently high, we will have:

$$\sigma_1 \geq \cdots \geq \sigma_m \geq \sigma_{m+1} \geq \cdots \geq \sigma_{M+1} \qquad (3.26)$$

where $\sigma_{m+1} \dots \sigma_{M+1}$,are nonzero only because of the nonzero noise term. Thus, some effects of the noise can be eliminated by replacing Σ by Σ' defined as

$$\Sigma' = \begin{bmatrix} \sigma_1 & \dots & 0 \\ \ddots & \dots & \vdots \\ \vdots & \sigma_n & \vdots \\ 0 & \dots & 0 \end{bmatrix}_{(N-M-1)x(M+1)} \qquad (3.27)$$

for some value of n satisfying m$\leq n \leq M + 1$(we will discuss ways of choosing n below). Finally, the vector $\hat{a} = [1\,\hat{a}_1 \dots \hat{a}_M]^T$ is found by solving

$$U\Sigma' V^I \hat{a}_M = 0$$

(3.28)

3.8 Estimation of Modal Amplitudes

Once we have estimates of the *A(z)* polynomial coefficients, we can find the corresponding zeros p_i by using a polynomial root finding method. It then remains to find the corresponding amplitude (d_i) coefficients. From equation (2.4) we can see that given the p_i, the problem of estimating the $d_i$is a linear one, so we can use a standard Least Squares approach. Of course we do not know the correct values of thep_i, but we can use the estimates obtained as described above in their stead. The least squares approach to estimating the d_i coefficients can be formulated as follows:

$$\begin{bmatrix} \hat{p}_1^0 & \cdots & \hat{p}_M^0 \\ \vdots & \vdots & \vdots \\ \hat{p}_1^{N-1} & \cdots & \hat{p}_M^{N-1} \end{bmatrix} \begin{bmatrix} \hat{d}_0 \\ \vdots \\ \hat{d}_{N-1} \end{bmatrix} - \begin{bmatrix} y_0 \\ \vdots \\ y_{N-1} \end{bmatrix} = 0 \qquad 3.29)$$

Where:

$\hat{p}_i$ are the estimates obtained from the first step. This equation is simply (3.1) written out in matrix form. Since the equation (3.9) is over determined, we can solve it in a least squares sense.

3.9 Elimination of Spurious Zeros

In previous sections we computed an estimate of a polynomial $A_M(z)$ of order $M > m$, and a corresponding set of M zeros $\{p_i\}_{i=1}^{M}$. We also computed amplitudes corresponding to these zeros. The next step is to separate the *m* zeros that correspond to the radar target (signal zeros) from the remaining spurious zeros [10].

The best criterion is based on the observation that a zero with modulus greatly different from one will influence only the data elements at the start (if the modulus is smaller than one) or at the end (if it is greater than one) [10]. In the time domain, we observe that such zeros correspond to widely distribute scattering centers, which are of little interest to radar target identification. Results of applying this zero selection method on buried target data shows two undesirable characteristics. First, this criterion produces erratic changes in the selected zeros as one changes the value of *m*. This is undesirable for RTI applications because our experience has shown that one needs to select the order differently for different target. Therefore, it is necessary for the order to be selected on-line, and thus we need algorithms that will produce similar estimates even if the order selected for the noisy data differs from the order selected for the catalog prototype. Second, the experimentally found spread of the resulting $d_i$and p_i parameters was such as to make them useless for classification: there were no clear clusters for the different targets. Hence, we needed a better way to differentiate spurious zeros from the signal zeros. We are currently investigating two different techniques, as detailed below.

The first technique is a refinement of the method in [10]. Whereas in [10] we kept all zeros within an ring around the unit circle with outer radius r and inner radius $\frac{1}{r}$, we now choose the outer and inner radii of the ring independently. In particular, since one expects spurious zeros to lie inside the unit circle when using backward prediction equations [4], the inner radius is set much closer to the unit circle than the outer one.

The second technique relies on the observation that since the spurious zeros correspond to modes that are not present in the data, their estimated energy should be low. To take advantage of this property, the algorithm is modified as follows. First, all M zeros are kept, and the amplitudes $\{d_i\}_{i=1}^{M}$corresponding to those zeros are found using equation (3.9). Then, the energy of each mode is computed using equation (2.8). The m zeros whose corresponding energy is the highest are kept and the remaining ones are discarded. Then, the energy estimates for the m kept zeros can be refined by re-computing the amplitude estimation using (3.9) with only the m selected zeros, however, since the energies for the discarded zeros is low, the difference between the two estimates should generally be small, so this refinement step may be omitted.

CHAPTER FOUR

SCATTERING CENTRE EXTRACTION ALGORITHM

4.1 Electromagnetic Scattering

Electromagnetic waves are one of the best known and most commonly encountered forms of radiation that undergo scattering. Scattering of light and radio waves (especially in radar) is particularly important. Several different aspects of electromagnetic scattering are distinct enough to have conventional names. Major forms of elastic light scattering (involving negligible energy transfer) are Rayleigh scattering and Mie scattering. Inelastic scattering includes Brillouin scattering, Raman scattering, inelastic X-ray scattering and Compton scattering.

Light scattering is one of the two major physical processes that contribute to the visible appearance of most objects, the other being absorption. Surfaces described as white owe their appearance to multiple scattering of light by internal or surface in homogeneities in the object, for example by the boundaries of transparent microscopic crystals that make up a stone or by the microscopic fibers in a sheet of paper. More generally, the gloss (or luster or sheen) of the surface is determined by scattering. Highly scattering surfaces are described as being dull or having a matte finish, while the absence of surface scattering leads to a glossy appearance, as with polished metal or stone.

Spectral absorption, the selective absorption of certain colors, determines the color of most objects with some modification by elastic scattering. The apparent blue color of veins in skin is a common example where both spectral absorption and scattering play important and complex roles in the coloration. Light scattering can also create color without absorption, often shades of blue, as with the sky (Rayleigh scattering), the human blue iris, and the feathers of some birds [12]. However, resonant light scattering in nano-particles can produce many different highly saturated and vibrant hues, especially when surface plasm on resonance is involved [20].

Models of electromagnetic energy scattering can be divided into three domains based on a dimensionless size parameter, α which is defined as:

$$\alpha = \frac{\pi D_p}{\lambda} \qquad (4.1)$$

Where $\pi D_p$the circumference of a particle and λ is is the wavelength of incident radiation. Based on the value of α, these domains are:

α ≪ 1: Rayleigh scattering (small particle compared to wavelength of light);

α ≈ 1: Mie scattering (particle about the same size as wavelength of light, valid only for spheres);

α ≫ 1: geometric scattering (particle much larger than wavelength of light).

Scattering centers extracted from radar returns are features that can be used for Automatic Target Recognition (ATR).Many different algorithms exist which can extract scattering centers from a radar return. They all, however, fall into one of two techniques used to estimate the signal parameters which are stated, described and categories as parametric and non-parametric methods in chapter three. In this thesis we are going to deals only with Parametric signal modeling to model and extract scattering center of buried Landmine targets.

4.2 Pole Determination

So far, it has been assumed that the signal associated with k^{th} scattering center can be defined by the k^{th} component of the prony model given in 4.2:

$$S_k(n) = a_k P_k^n \qquad (4.2)$$

The complete construction of the model requires determination of the value of the amplitude coefficients a_k and those of the poles p_k for every scattering center here; we examine linear prediction methods based on the super resolution algorithms matrix pencil.

This method is called the matrix Pencil (MP) [2].This more recent method is also known as "generalized pencil of functions" (GPOF) due to the fact that it determines the poles by solving a generalized eigen value problem.

4.2.1 Matrix Pencil

This section concerns with linear prediction technique known as the matrix Pencil (MP) [2]. In linear algebra, a Hankel matrix, named after a Herman Hankel, is a square matrix in which each ascending skew-diagonal from left to right is constant.

The Matrix pencil method solves a generalized Eigen value problem. The techniques can also exploit subspace decomposition and the rank deficiency of Hankel matrices. The following presents the principle of SVD matrix Pencil for the extraction of cisoids [3][4].

The matrix pencil is a linear combination of two matrices, $H_1 - zH_2$ where H_1 and $H_2$are formed from the prediction matrix H presented in 4.3.

$$H_1 = \begin{bmatrix} x_{(0)} & x_{(1)} & \cdots & \cdots & x_{(L-2)} \\ x_{(1)} & x_{(2)} & \vdots & \vdots & \vdots \\ \vdots & \vdots & \vdots & \vdots & \vdots \\ \vdots & \vdots & \vdots & \vdots & \vdots \\ x_{(R-1)} & \cdots & \cdots & \cdots & x_{(N-2)} \end{bmatrix} \qquad (4.3)$$

$$H_2 = \begin{bmatrix} x(1) & x(2) & x(3) & \dots & x(L-1) \\ x(2) & x(3) & \vdots & \vdots & \vdots \\ x(3) & x(4) & \vdots & \vdots & \vdots \\ \vdots & \cdots & \vdots & \vdots & \vdots \\ x(R) & \cdots & \cdots & \cdots & x(N-1) \end{bmatrix} \qquad (4.4)$$

Where: L is the pencil parameter that determines the dimensions of the space.

The matrices can be decomposed as follows:

$$H_1 = Z_1.B.Z_2 \quad .... 4.5$$

$$H_2 = Z_1.B.Z_0.Z_2 \quad ....4.6$$

Where

$$Z_1 = \begin{pmatrix} 1 & 1 & \dots & 1 \\ Z_1 & Z_2 & \dots & Z_m \\ Z_1^{N-L-1} & Z_2^{N-L-1} & \dots & Z_m^{N-L-1} \end{pmatrix} \qquad (4.7)$$

$$Z_2 = \begin{pmatrix} 1 & Z_1 & \dots & Z_1^{L-1} \\ 1 & Z_m & \dots & Z_m^{L-1} \end{pmatrix} \qquad (4.8)$$

and

$$Z_0 = diag(Z_1, Z_2, \dots, Z_m) \qquad (4.9)$$

$$B = diag(b_1, b_2, \dots, b_n) \qquad (4.10)$$

Where diag [•] denotes a M ×M diagonal matrix.

The matrix pencil can then be written

$$H_1 - zH_2 = Z_1 B(Z_0 - zI)Z_2 \qquad (4.11)$$

Where, I is the M ×M identity matrix.

Each observation matrix can be decomposed into a signal matrix, S, and a perturbation matrix, E. The pencil of the matrix can be decomposed as a sum of signal and noise matrices, S and E, respectively. It follows that a new expression of the pencil of matrix is given in 3.61.

$$H_1 - zH_2 = (S_1 + E_1) - z(S_2 + E_2) \qquad (4.12)$$

$$= (S_1 - zS_2) + (E_1 - zE_2) \qquad (4.13)$$

In 3.61, S_1 *and* S_2 have the same column space and the same row space. One can demonstrate that the rank of the matrix pencil will be M, provided that M < L < N − M. However, if {z = zi; i = 1, . . . ,M}, the ith row of (Z0 − zI) is zero, and the rank of this matrix is M − 1. In other words, the noiseless pencil S1 − z.S2 decreases its rank by one if and only if z is one of the generalized eigen-values (GE) of H1 − z.H2.

Hence, we know the poles are the generalized Eigen-values of the matrix pair [H1;H2]. However, the direct computation of the GE is not stable because S1 and S2 are not full rank. It is common to replace the matrices H by their truncated SVD's. The truncated versions are denoted by H1T and H2T and 7→ denotes the rank-P SVD truncation.

$$H_1 \mapsto H_1T = U_1 \Sigma_1 V_1^H \qquad (4.14)$$

$$H_2 \mapsto H_2T = U_2 \Sigma_2 V_2^H \qquad (4.15)$$

Where U_1, Σ_1 *and* V_1 only contain the P principal elements.

Replacing the truncated matrix into the matrix pencil yields

$$H_{1T} - zH_{2T} = U_2^H U_1 V_1^H V_2 - zE_2 \qquad (4.16)$$

The poles can be estimated by computing the eigen-values of 3.64 or equivalently the eigen-values of (4.15).

$$\Sigma_2^{-1} U_2^H U_1 \Sigma_1 V_1^H V_2 = [H_{2T}^H H_{1T}]^{-1} \, [H_{1T}^H H_{2T}] \qquad (4.17)$$

Figure 4.1 represents the poles of H determined by the Matrix Pencil **-N = 64, P = 3, L = 22, SNR= 30 dB**.

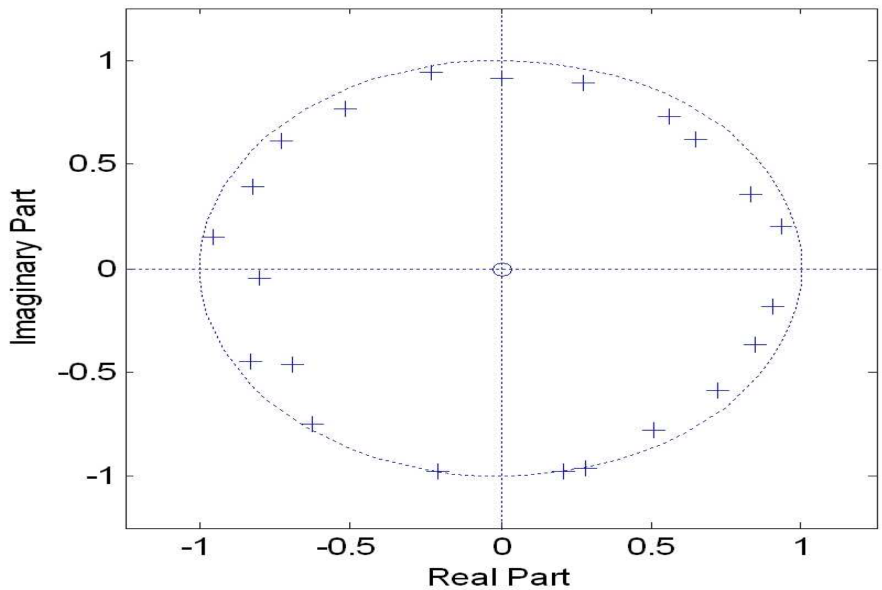

Figure 4. 1. Z-plane - poles obtained with the Matrix Pencil

4.3 Geometrical theory of diffraction

In 1953, Keller introduced the geometrical optics theory of diffraction as an extension to geometrical optics to include edge and vertex diffracted rays. He then developed his theory for the field of rays diffracted from a perfectly conducting wedge. The method is known as the Geometrical Theory of Diffraction (GTD). It predicts that at high frequency, the incident field appears to originate from a discrete set of independent scattering-centres and follows a $(jk)^{\alpha}$ frequency dependence where α depends upon the target geometry. For an incident field that is an infinite plane wave, the model for the geometrical theory of diffraction is given by (3.16) [5].

$$E(f) = \sum_{m=1}^{M} A_m \left\{ j \frac{f}{f_c} \right\}^{\alpha_m} e^{-j\frac{4\pi}{c} r_m} \qquad (3.18)$$

Where

A_m is the complex amplitude associated with the reflectivity of the m^{th} scattering-centre f frequency

f_c reference frequency

r_m relative location of the A_m scattering-centre,

α_m frequency dependence parameter of the m^{th} scattering-centre.

For simple targets, the frequency dependence of canonical scattering geometries is given by the following table [6].

4.4 High-frequency approximation

In the high-frequency region where most radar systems operate, it is often assumed that man-made targets can be accurately represented by a set of isolated scattering points. These scatterers generally correspond to discontinuities on the target. Due to structural similarities, scattering points on similar landmines are principally located in the same areas. They principally include case materials, shape and internal materials.

Let a target be composed of P scattering centers. Providing there are no strong interactions between the scattering-centers, the signal, s(n), could be approximated by a sum of P complex exponentials.

$$s(n) = \sum_{p=1}^{P} a_p z_p^n \qquad (4.19)$$

Where the complex coefficient, a_p , and the pole, $z_p = \rho_p e^{i.\varphi_p}$, are associated with the reflectivity and the location of the P^{th} scattering-center, respectively. Let us assume that amongst the P scattering-centers, M is much stronger than the others. In this case, the signal can be approximated with the contributions of M scatterers. It follows

$$s(n) = \sum_{p=1}^{M} a_p z_p^n + \sum_{p=M+1}^{P} a_p z_p^n \quad P > M \qquad (4.20)$$

$$s(n) = s_1(n) + s_2(n) \approx s_1(n) \quad \forall(M, n)) \text{ /Power (s1)} \gg \text{Power (s2)}$$

Figure 4.2 illustrates the concept of scattering-centers for an aircraft. Strong scatterers on the target are projected onto the direction of propagation of the beam, x.

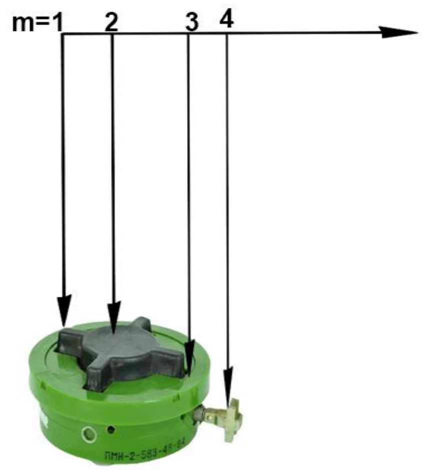

Figure 4. 2. Concept of scattering-centers in one-dimensional imaging on the

4.5 Scattering Center Extraction

In 1795, Prony developed a polynomial-based prediction method for modeling a sum of complex exponential signals [13]. The introduction of Least- Squares methods in the 1970's enables accurate pole extraction to be achieved more efficiently. However, these algorithms are also extremely sensitive to the noise. In 1978, Kung introduced a state-space method for harmonic retrieval directly from the data [25]. The eigenvectors of the autocorrelation matrix are obtained by singular-value-decomposition (SVD) rather than by computing the autocorrelation matrix itself. Four years later, Tufts and Kumaresan developed the principle for estimating the parameters of exponentially damped sinusoids [49]. This eigenvector method (or principal eigenvalue method) reduces the effect of noise by only using the set of eigenvectors that constitute a basis for the signal subspace. For low signal-to-noise ratios, these methods are known to perform better than any other method based on Least-Squares approach. In 1987, a new version of the Prony method was proposed by Rahman and Yu, Total Least-Squares (TLS-Prony) [39]. An alternative to these polynomial methods commenced with the creation of more recent techniques such as ESPRIT [34] and Matrix Pencil [17]. Based on the Generalised-Eigenvalue approach, they also achieve accurate linear prediction for low signal-to-noise ratio conditions.

In this section, we are interested in a linear prediction technique that relies on the construction of a scattering model defined as a finite sum of complex exponentials, known as cisoids. The technique is employed to demonstrate that a scattering model can improve radar range-resolution. Firstly, the signal backscattered from three simulated spheres is modeled by three point-scatterers. Secondly, the model is determined by a linear-prediction technique, which consists of five processing stages:

Model-order estimation

Pole determination

Pole selection

Amplitude coefficient estimation parameter adjustment.

The model is then extrapolated across a large bandwidth. Whereas the initial signal can only generate two peaks on the range-profile, the extrapolated model enables the third to be resolved. Several algorithms can be used for computing each stage. This section offers an insight into some of them.

4.6 Model Order Selection

The model-order is the number of terms in the model used by linear prediction methods. Here, the model-order of the autoregressive process corresponds to the number of scattering-centers, P, that contribute to the signal. Estimating the model-order is needed for building the model. Even if the number of targets is known, the model-order has to be estimated because the enhanced resolution may increase the number of scattering-centers that may become relevant.

4.6.1 Singular-Values

It is possible to estimate the model-order by exploiting the multiplicity of the eigen-values that are related to the noise. Here, the eigen-values are estimated by singular-value-decomposition (SVD) of the matrix H. Because the singular-values are directly related to the eigen-values, the L−P smallest singular-values, should have small and almost identical values related to the power of the noise.

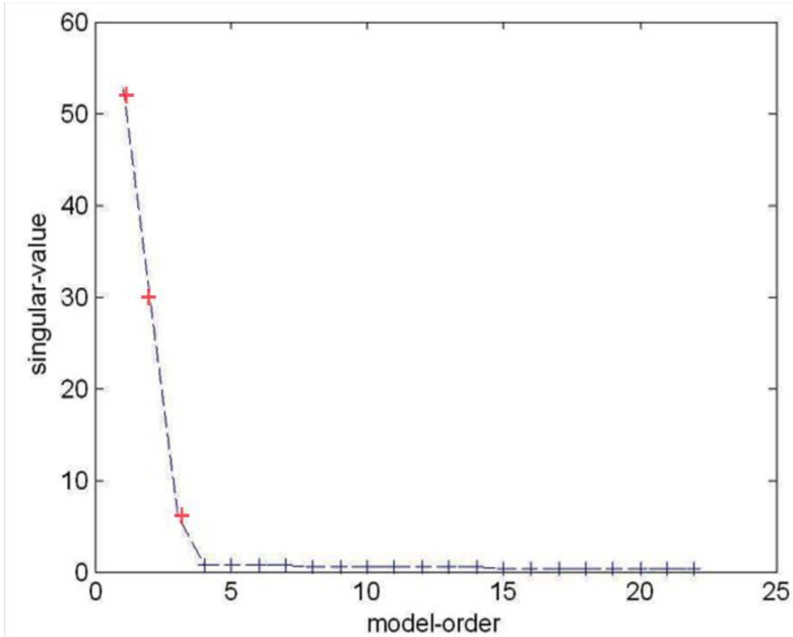

Figure 4. 3. Model-order estimation

Figure 4.3 represents the singular-values extracted from the first N=64 complex-valued radar-signals. For L = 22, the nineteen weakest singular-values, directly related to the power of the noise, can be easily identified. For SNR = 30 dB, the transition between groups of singular-values suggests that the model-order is M = 3.

4.7 Pole Selection

Regardless of the method chosen, the set of poles computed always comprise poles that are not associated with any physical scattering centers. It is thus essential that only "true poles "be selected and inserted in the model. The spatial distribution of the scattering center is related to the magnitude p_k of the pole estimated for that center. If p_k is too far from the unit circle then its contribution to the frequency model is greatly different at frequency f_0 and at frequency f_{N-1} . So, the true poles are the p poles whose modulus is close to one that is those lying on the unit - circle. For an unknown number of scattering centers, Carriere and Moses suggest criteria for discarding spurious poles [1].

$$\frac{1}{100} < |P^N| < 100 \qquad 4.21$$

Expressions 4.20 and 4.21 are numerical examples of boundaries for 64 and 128 samples.

$$0.93 < |P| < 1.07 \text{ ,N=64} \qquad 4.22$$

$$0.96 < |P| < 1.03 \,, N = 128 \qquad 4.23$$

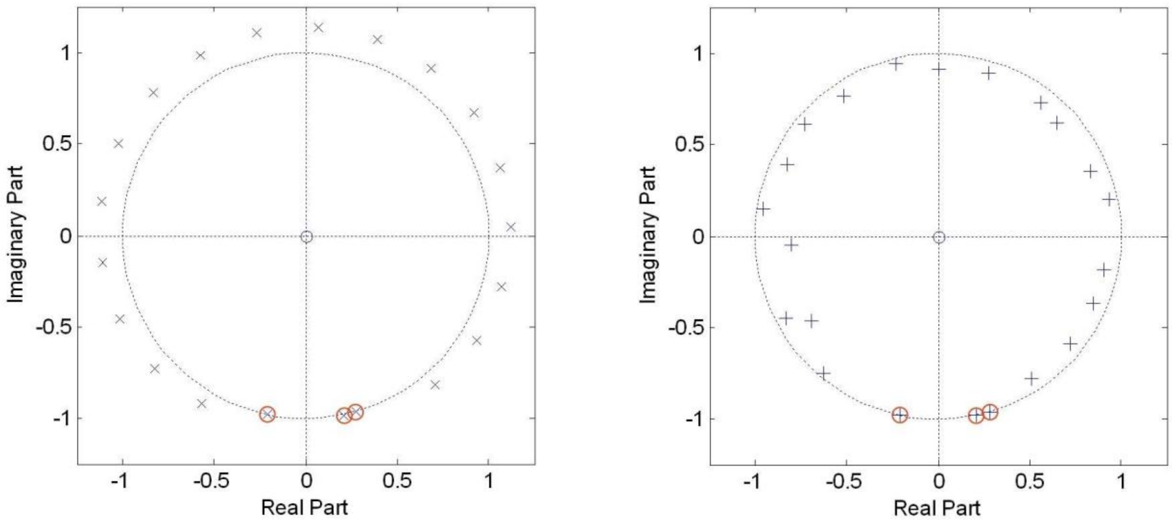

Figure**4. 4.** Shows the poles selected using the above criterion.

4.8 Matching Algorithm Using Cluster Approach in Z Plane

4.8.1 Matching Algorithms

The fundamental computational operation performed by the radar system is to match an incoming test signature against a library of pre-recorded signatures [4]. In order to evaluate matching algorithms efficiently, we utilize the pole signal in z plane for the four different buried target's signatures .In this thesis we have used Euclidean Distance (ED) matching algorithm to compute a single match value when executed on a library signature and test signature pair. The pole corresponding to the library signature that exhibits the best match with the test signature is selected. For Euclidean Distance, the total distance between the two signatures is calculated by taking the square root of the sum of squared differences. The match with the smallest total difference is taken as best.

The Euclidean distance between points p and q is the length of the line segment connecting the them ($\overline{pq}$). In Cartesian coordinates, if p= $(p_1, p_2, p_3, \dots p_n)$ and q=$(q_1, q_2, q_3, \dots q_n)$ are two points in Euclidean n-space, then the distance ((d_{Eu})) from p to q ,or from q to p is given by the following formula (r2).

$$d_{Eu}(p,q) = \sqrt{(p_1 - q_1)^2, (p_2 - q_2)^2, \dots, (p_n - q_n)^2} \qquad 4.24$$

In polar coordinates Euclidean distance can be expressed as follow if the point **p** are (r_1, θ_1) those of q are ((r_2, θ_2),then the distance between the points is

$$d_{Eu}(p,q) = \sqrt{r_1^2 + r_2^2 - 2r_1 r_2 \cos(\theta_1 - \theta_2)}$$

Euclidian distance: $d_{Eu} = \left(\sum_{i=1}^{p} d_i^2\right)^{\frac{1}{2}}$ 4.25

where d_i is the inter-pole distance corresponding to a cluster C_i.

4.8.2 Understanding Cluster Analysis

Cluster analysis is a convenient method for identifying homogenous groups of objects called clusters. Objects (or cases, observations) in a specific cluster share many characteristics, but are very dissimilar to objects not belonging to that cluster.

The objective of cluster analysis is to identify groups of objects or property (in this case, poles) that are very similar with regard to their magnitude and angle and assign them into clusters. After having decided on the clustering variables (pole angle and magnitude), we need to decide on the clustering procedure to form our groups of objects. This step is crucial for the analysis, as different procedures require different decisions prior to analysis. K-Means algorithm is an unsupervised clustering algorithm that classifies the input data points into multiple classes based on their inherent distance from each other [48]. So in this thesis K-Means algorithm technique is used for grouping the most similar objects into a cluster and to determining each object’s cluster membership. In other words, whereas an object in a certain cluster should be as similar as possible to all the other objects in the same cluster, it should likewise be as distinct as possible from objects in different clusters. Some approaches most notably hierarchical methods require us to specify how similar or different objects are in order to identify different clusters. Most software packages calculate a measure of dissimilarity by estimating the distance between pairs of objects. Objects with smaller distances between one another are more similar, whereas objects with larger distances are more dissimilar.

An important problem in the application of cluster analysis is the decision regarding how many clusters should be derived from the data. This question is explored in the next step of the analysis. Sometimes, however, we already know the number of segments that have to be derived from the data.

Table4. 1.Test and Template poles

Simulation		
Pole	**Test poles**	**Template poles**
p_1	-0.02 + j0.18	-0.0196 + j0.1796
p_2	-0.02 - j0.18	-0.0196 - j0.1796
p_3	-0.01 + j0.10	0.0079 + j0.1796
p_4	-0.01 - j0.10	0.0079 - j0.1796

4.8.3 Cluster Selection

For two patterns of M and M′ poles, the total number of different clusters is MxM′. For two patterns of M true poles, the number of possible unsorted arrangements of M clusters is M! but more likely, the number of arrangements that make physical sense is smaller. For example, it can decrease if:

1. The patterns contain spurious poles that were not rejected by the filter
2. The patterns contain true poles that do not appear on both due to small variations of the conditions of measurements.

The total number of possible unsorted combinations of K clusters is given by $N_{comb}(K)$ in (4.26)

$$N_{comb}(K) = \frac{1}{K!}\frac{M!M'!}{(M-K)!(M'-K)!} \qquad 4.26$$

Where: (K < M) and (K < M′).

For reducing the computation time, a number of combinations can be discarded based on the fact that some combinations of poles and some combinations of clusters are not likely to correspond to physical situations. For instance, poles that are located in different half-planes are not likely to correspond to the same scatterer. Mathematically, this can be regarded as the rejection of the clusters which by themselves would increase the distance between patterns beyond any typically acceptable limits. Similarly, since the target is assumed to be rigid, poles ordered by increasing angles are not likely to correspond to poles that are not.

Figure 4.5 illustrates the clustering approach using a combination of three pairs of poles obtained for M = 5 and M′ = 6. The poles are represented by different markers: (×) for the test-pattern and (+) for the template-pattern.

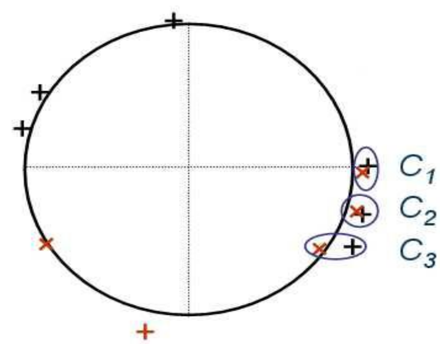

Figure 4. 5. Concept of pole clustering for K = 3, M = 5 and M′ = 6.

4.8.4 Z-Domain Classification

Z-Domain classification is achieved by comparing radar-signals based on features that are visible in the pattern of poles in the z-plane; where the pole is being related to the scattering function.

The classification technique introduced in this chapter is based on the idea that the poles of the model parameters are less sensitive to noise and small variation of aspect-angles than the reconstructed model. It reveals that radar-measurements involving similar targets and similar perspectives should present similarities that can be observed in the pattern of poles expressed in the z-plane. As this is a key requirement for classification, it is believed that a signal could be classified by comparing its pattern of poles with other pole template-patterns in library. Physically each measurement is classified based on the probability that the target shares a common arrangement of scatterers in range with other targets in library.

This section presents the principle of classification of targets based on the pattern of poles.

In order to present the principle of these classification techniques, let us start by considering two true poles, z_k and z'_m on the test-pattern and the template-pattern, respectively. Assuming that the patterns are aligned, the pole-angles correspond to the same absolute time-delay. One can thus estimate that these poles are associated with two scatters that induce the same time-delay if the interpole-distance, d($z_k; z'_m$) is null.

Considering that the poles chosen are directly related to the location of the scatters, one can consider that the classification technique proposed is strongly based on the spatial arrangement of the scatters on the target. In other words, the technique relies on the assumption that similar arrangements of the scatters on the targets yield similar arrangements of the true poles in the z-plane. For two successive measurements of the same target, it is expected that some elements of the pole patterns coincide.

The technique proposed for classifying targets is a matching algorithm using a clustering approach in the z-plane (MAUCAZ). Signals are classified by comparing their patterns of poles with templates in a library. A limited number of clusters are formed by associating two poles, one from the test-pattern and the other from the template-pattern, supposedly related to the same physical scatter on the target. The similarities between two patterns are quantified by means of a mathematical expression that increases with the distance between corresponding poles. This method enables the classifier to take into account the variations of the poles mentioned above.

Although the whole pattern of poles represents a source of information, it is chosen to focus on the poles that correspond to physical scatterers. It is believed that by taking enough poles into account, their values can provide sufficient information to distinguish between the limited number of potential targets. The principal task of feature selection is to identify the poles that are relevant for classification. It consists of separating the elements, called true poles, which are related to physical scatterers, from the other elements considered as artefacts.

For a target composed by P scatterers, removing the extraneous poles is conventionally achieved by keeping the P poles that are the closest to the unit-circle. In this case, all the filtered patterns would have the same number of poles.

These boundaries define a selective filter whose transfer function can be represented as a ring in the z-plane. Figure 4.6 shows the principle of pole pre-selection. The figure on the left-hand side represents the L − 1 poles in the z-plane. The poles selected by the filter belong to the area represented in blue. The figure on the right-hand side represents the resulting pattern of poles as it appears in the feature-selection stage.

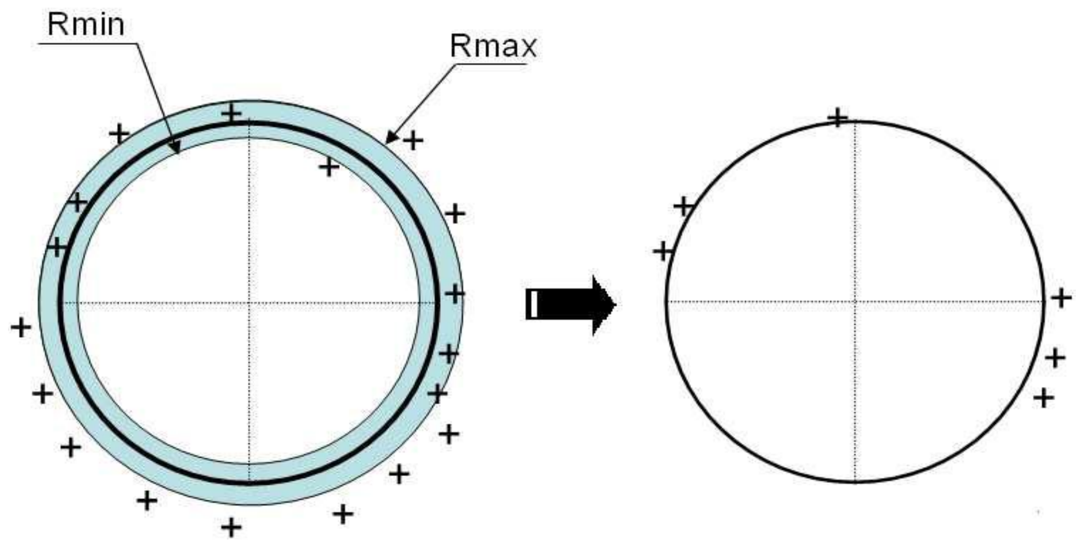

Figure 4. 6. Concept of MAUCAZ

4.8.5 MAUCAZ

The classifier is based on the principle that two targets sharing similar arrangements of scatterers also share similar arrangements of the poles in the z-plane. Classification can thus be described as gathering the template patterns whose K poles have a high probability, $P(K) \gg PK$, to correspond to K scatterers related to K poles of the test-pattern. Identification is achieved when a class is populated by one template only.

It appears that the arrangement of poles into clusters is an important aspect of the classification. However, for a given template, there is a priori no robust rule stating what are the couples of poles that should be combined to form clusters.

Assuming that there exists in the library a measurement carried out on the same type of target and at similar aspect-angle as the test-measurement, it is expected that most true poles of the test-pattern coincide with the true poles of the template-pattern since they are associated with the same scatterers. The problem of recognition consists of finding, in each pattern, the arrangement of K pairs of poles that “match” each other.

The first stage consists of computing the inter-pole distance for all possible clusters, $C_{k,m}$, whose poles, z_k and $z_m^{'}$, are obtained from the test-pattern and from the template-pattern, respectively. Figure 4.7 represents the array containing the interpole distance, D(k,m), obtained using one of the expressions proposed. Each row corresponds to a pole, z_k, in the test-pattern and each column to a pole, $z_m^{'}$, in a template-pattern Cluster Selection

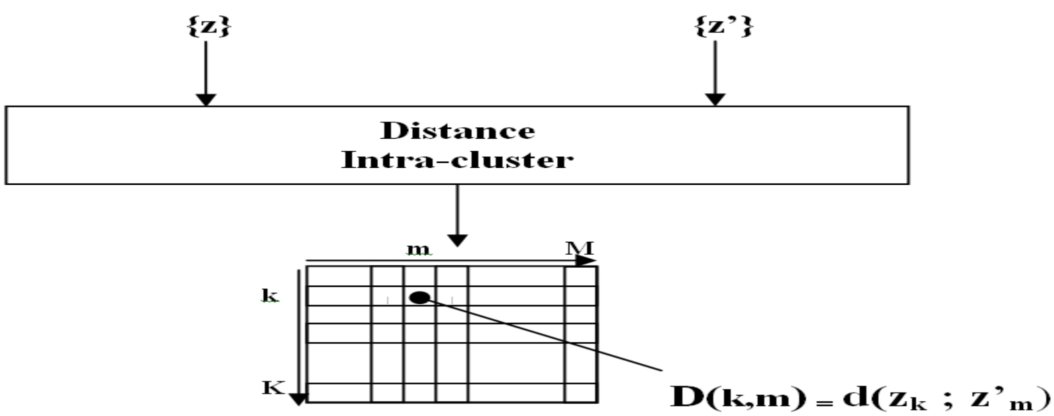

Figure 4. 7. MAUCAZ: computation of the inter-pole distances

The second stage involves comparing the levels of similarity between the test-pattern and the templates patterns in library. The ’best-matching pattern’ is not found by computing the probability itself but using the expressions of the distance between patterns proposed. The minimum distance is expected to occur when the selected clusters are formed by poles that Correspond to the same scatterer as it is the most likely solution.

Since the corresponding poles cannot be easily identified, it is proposed to consider all the possible combinations of poles that can be used to create K clusters. For each, it is proposed to find the arrangement of K clusters that has the highest probability that the K clusters be formed by poles associated with scatterers at the same range and with geometries leading to the same energy spread in the range.

CHAPTER FIVE

DESIGN AND IMPLEMENTATION

The overall system model in this thesis has incorporated the following two major steps: scatteing center extraction algorithm and Matching Algorithm Using Cluster Approach in Z plane. The high level view of the overall system is shown in Fig 6.1.

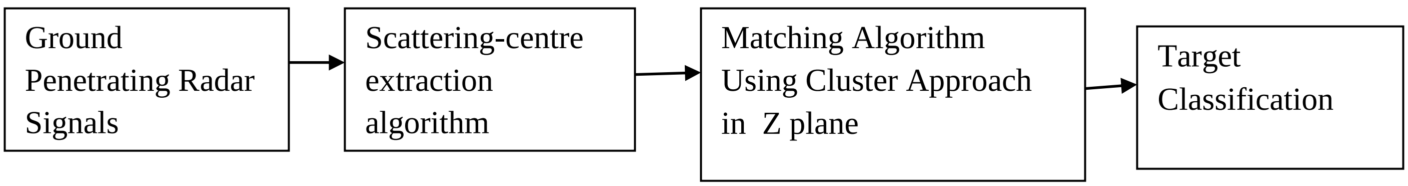

Figure 5. 1.General Scheme of the Design

5.1 GPR Data Acquisition

The Ground Penetrating Radar, which is used to obtain the data in this thesis, is a stepped frequency waveform with operating frequency of 100MHz to 5GHz. Dry Sand soil is selected as host medium and PMN2 Land mine as Buried Land mine with Plastic and metallic case material is considered.

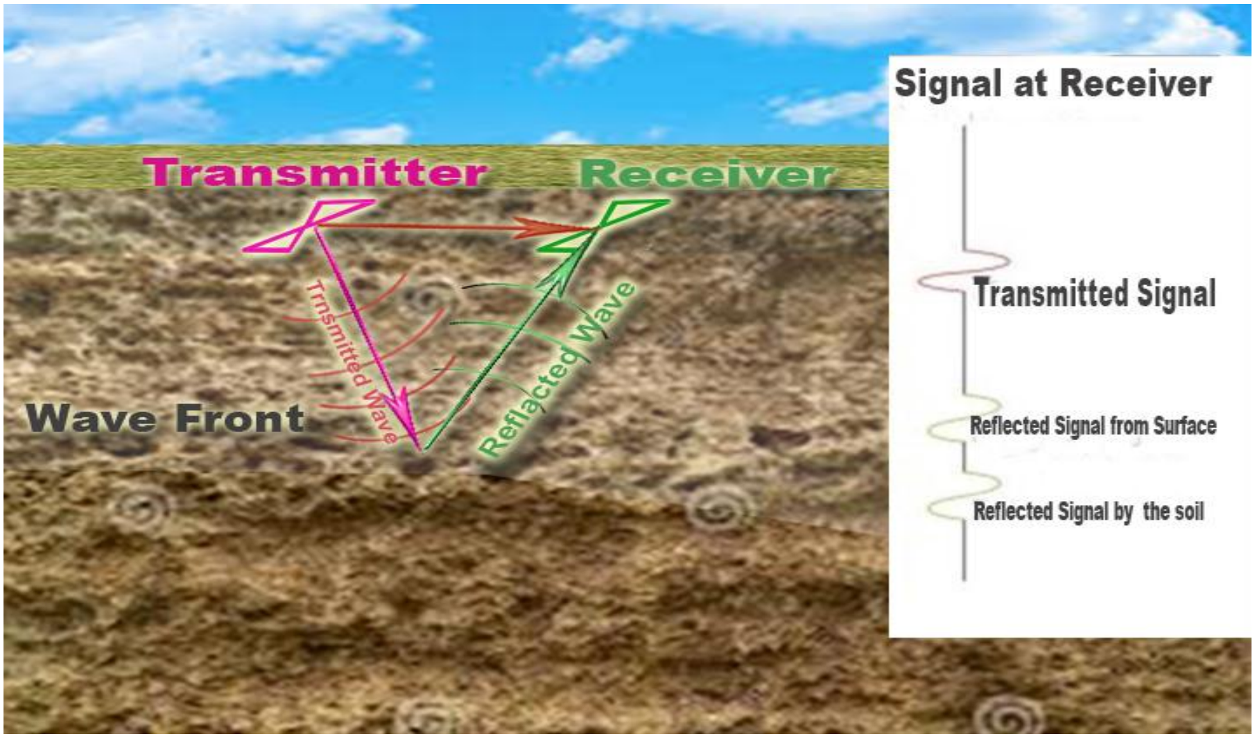

Figure5. 2. A diagram of how the electromagnetic wave is transmitted and reflected without the target.

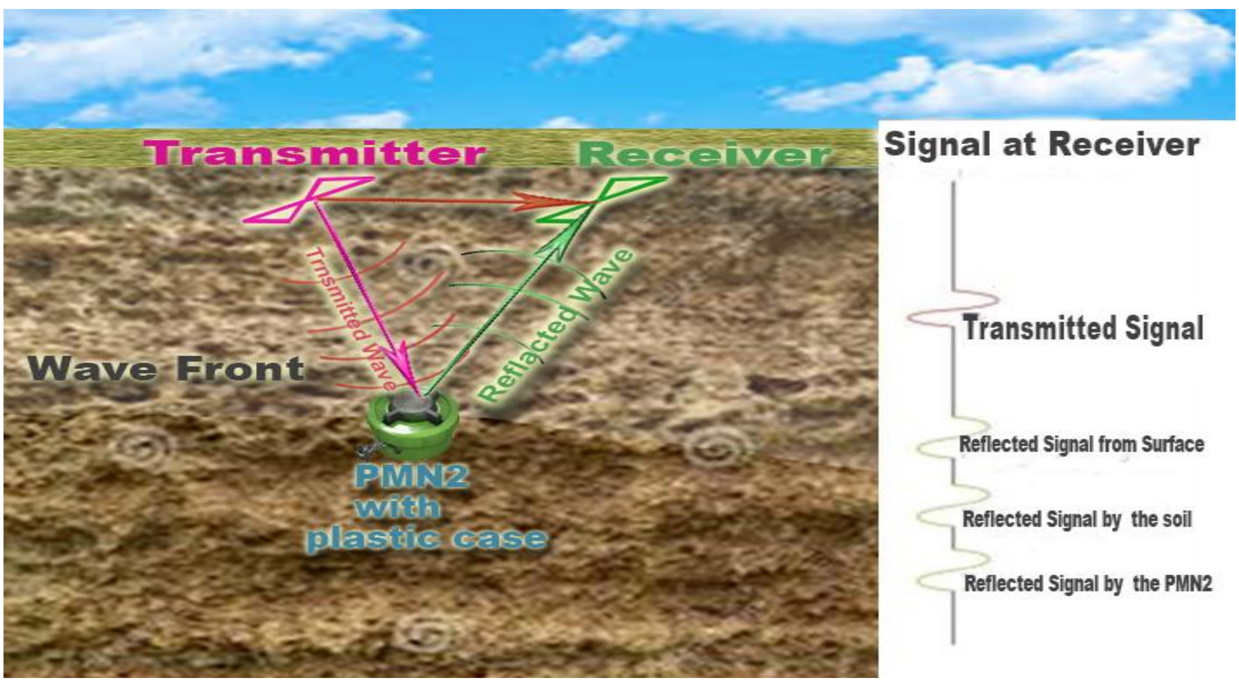

Figure 5. 3. A diagram of how the electromagnetic wave is transmitted and reflected with presence of the target with Plastic case.

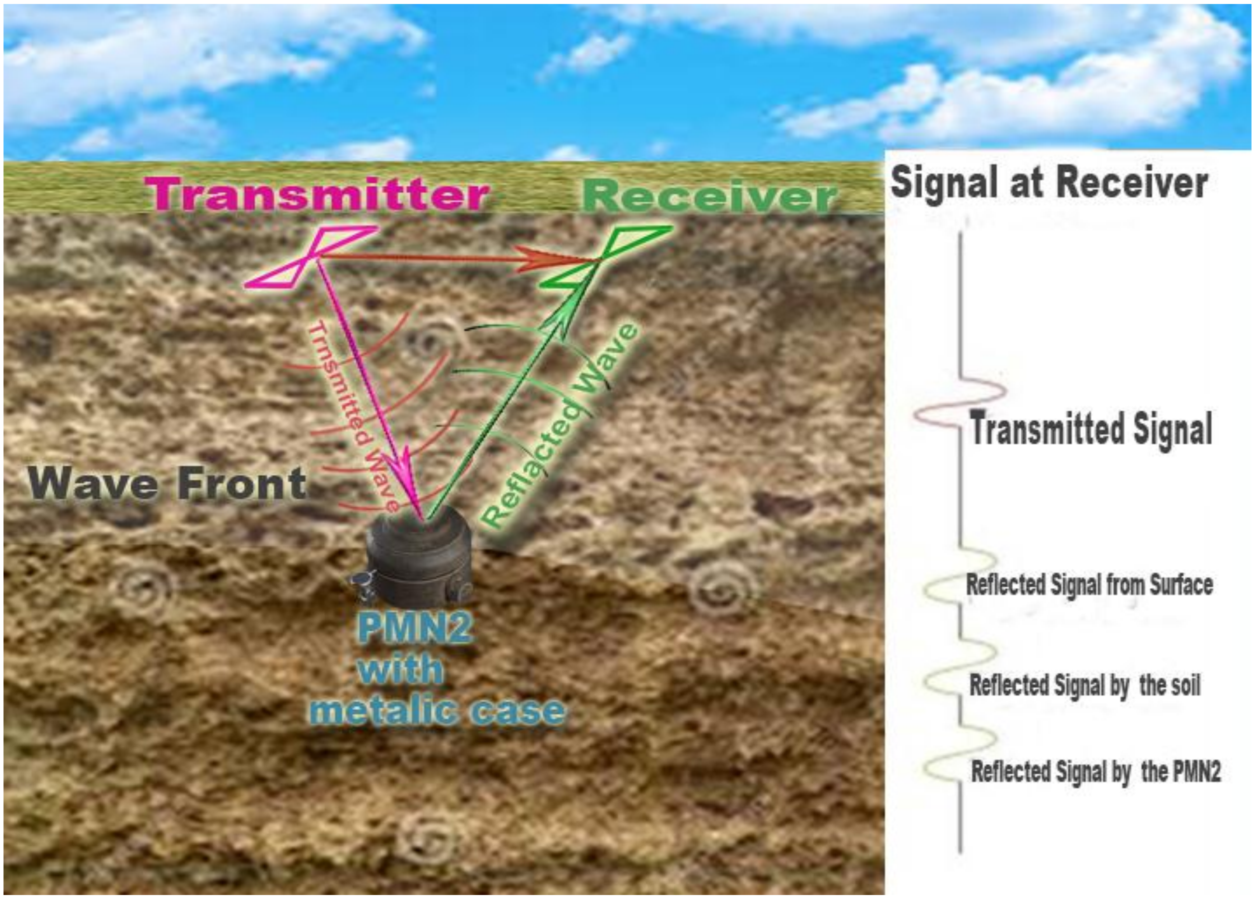

Figure5. 4. A diagram of how the electromagnetic wave is transmitted and reflected with presence of the target with Metallic case.

The propagation velocity v of the electromagnetic wave in soil is characterized by the Dielectric permittivity, ε and magnetic permeability , μ of the medium:

$$v = \frac{c}{\sqrt{\varepsilon_r}} \qquad (5.1)$$

The wavelength, λ is defined as the distance of the wave propagation in one period of oscillation and is obtained by

$$\lambda = \frac{v}{f} = \frac{2\pi}{\omega\sqrt{\varepsilon\mu}} \qquad (5.2)$$

In the plane Wave solution of Maxwell's equations, the electric field , E of an EM wave that is travelling in z- direction is expressed as

$$E(z,t) = E_0 e^{j(\omega t - kz)} \qquad (5.3)$$

Measurement with Ground Penetrating Radar for different Landmines

Figure.5.5. Detecting the Mine with Metal Detector

Figure.5.6. setting Up the GPR at site

Figure. 5.7.Taking Measurement with Ground Penetrating Radar at site

(a) (b) (c) (d)

Figure .5.8. Examples of APM; (a) PRB-M35, (b) PMN, (c) VALMARA-69, (d) MON-100

Table5.1. Specifications of the APM

Type	PRB-M35	PMN	VALMARA-69	MON-100
Dimension	H58mm,D64mm	H56mm,D112mm	H105mm,D130mm	H82mm,D236mm
Weight	158g	600g	3.3kg	5.0kg
case	Plastic	Rubber	Plastic	Steel
Sensitivity	8kg	8kg	10.8Kg directly ,6kg through trip wire	Depend on fuse
Lethal Range	---	---	Radius 27m	100m by 9.5m arc
Country of Origin	Belgium	Former Soviet Union	Italy	Former Soviet Union

Table.5.2. Measurement with PMN2 Mines in Dry sand soil at 100cm depth

R.N	Measurement	Number of model order	Complex conjugate poles	Amplitude coefficient
1	measurement in sand soil without the mine presence	2	$s_1 = -0.04 + j0.22$ $s_2 = -0.04 - j0.22$	$C_1 = 2000 + j3$ $C_2 = 2000 - j3$
2	Measurement done with PMN2 mine before buried in sand soil	4	$s_1 = -0.02 + j0.2$ $s_2 = -0.02 - j0.2$ $s_3 = -0.008 + j0.1$ $s_4 = -0.008 - j0.1$	$C_1 = 4000 + j6$ $C_2 = 4000 - j6$ $C_3 = 200 + j1500$ $C_4 = 200 - j1500$
3	Measurement done with PMN2 buried at 100cm in sand soil	6	$s_1 = -0.04 + j0.22$ $s_2 = -0.04 - j0.22$ $s_3 = -0.02 + j0.2$ $s_4 = -0.02 - j0.2$ $s_5 = -0.008 + j0.101$ $s_6 = -0.0081 - j0.12$	$C_1 = 18000 + j4$ $C_2 = 18000 - j4$ $C_3 = 18000 + j4$ $C_4 = 18000 - j4$ $C_5 = 100 + j3000$ $C_6 = 101 - j3020$

Table.5.3. Measurement with PRB-M35 Mines in Dry sand soil at 100cm depth

R.N	Measurement	Number of model order	Complex conjugate poles	Amplitude coefficient
1	measurement in sand soil without the mine presence	2	$s_1 = -0.04 + j0.22$ $s_2 = -0.04 - j0.22$	$C_1 = 2000 + j3$ $C_2 = 2000 - j3$
2	Measurement done with PRB-M35 mine before buried in sand soil	4	$s_1 = -0.101 + j0.11$ $s_2 = -0.101 - j0.11$ $s_3 = -0.027 + j0.21$ $s_4 = -0.027 - j0.21$	$C_1 = 2000 + j3$ $C_2 = 2000 - j3$ $C_3 = 100 + j3000$ $C_4 = 100 - j3000$
3	Measurement done with PRB-M35 buried at 100cm in sand soil	6	$s_1 = -0.06 + j0.4$ $s_2 = -0.06 - j0.4$ $s_3 = -0.022 + j0.2$ $s_4 = -0.022 - j0.2$ $s_5 = -0.108 + j0.10$ $s_6 = -0.108 - j0.10$	$C_1 = 2000 + j3$ $C_2 = 2000 - j3$ $C_3 = 2000 + j3$ $C_4 = 2000 - j3$ $C_5 = 100 + j3000$ $C_6 = 101 - j3020$

Table.5.4. Measurement with VALMARA-69 Mines in Dry sand soil at 100cm depth

R.N	Measurement	Number of model order	Complex conjugate poles	Amplitude coefficient
1	measurement in sand soil without the mine presence	2	$s_1 = -0.04 + j0.22$ $s_2 = -0.04 - j0.22$	$C_1 = 2000 + j3$ $C_2 = 2000 - j3$
2	Measurement done with VALMARA-69 mine before buried in sand soil	4	$s_1 = -0.02 + j0.2$ $s_2 = -0.02 - j0.2$ $s_3 = -0.008 + j0.1$ $s_4 = -0.008 - j0.1$	$C_1 = 4000 + j6$ $C_2 = 4000 - j6$ $C_3 = 200 + j1500$ $C_4 = 200 - j1500$
3	Measurement done with	6	$s_1 = -0.04 + j0.22$	$C_1 = 18000 + j4$

	VALMARA-69 buried at 100cm in sand soil		$s_2 = -0.04 - j0.22$ $s_3 = -0.02 + j0.2$ $s_4 = -0.02 - j0.2$ $s_5 = -0.008 + j0.101$ $s_6 = -0.0081 - j0.12$	$C_2 = 18000 - j4$ $C_3 = 18000 + j4$ $C_4 = 18000 - j4$ $C_5 = 100 + j3000$ $C_6 = 101 - j3020$

Table.5.5. Measurement with MON-100 Mines in Dry sand soil at 100cm depth

R.N	Measurement	Number of model order	Complex conjugate poles	Amplitude coefficient
1	measurement in sand soil without the mine presence	2	$s_1 = -0.04 + j0.22$ $s_2 = -0.04 - j0.22$	$C_1 = 2000 + j3$ $C_2 = 2000 - j3$
2	Measurement done with MON-100 mine before buried in sand soil	4	$s_1 = -0.06 + j0.3$ $s_2 = -0.06 - j0.3$ $s_3 = -0.01 + j0.1$ $s_4 = -0.01 - j0.1$	$C_1 = 4000 + j6$ $C_2 = 4000 - j6$ $C_3 = 200 + j1500$ $C_4 = 200 - j1500$
3	Measurement done with MON-100 buried at 100cm in sand soil	6	$s_1 = -0.08 + j0.2$ $s_2 = -0.08 - j0.2$ $s_3 = -0.05 + j0.23$ $s_4 = -0.05 - j0.23$ $s_5 = -0.001 + j0.11$ $s_6 = -0.001 - j0.11$	$C_1 = 18000 + j4$ $C_2 = 18000 - j4$ $C_3 = 18000 + j4$ $C_4 = 18000 - j4$ $C_5 = 100 + j3000$ $C_6 = 101 - j3020$

5.2 Vertical and Horizontal Resolution

For 2GHz center frequency Vertical and Horizontal resolution will be given as below:
Vertical resolution can be determined as below:

$$V_r = \frac{T_{pulse}.C}{2\sqrt{RDP}} \qquad (5.4)$$

Where:

V_r is the vertical resolution

T_{pulse} is the transmitted pulse duration, this can be calculated by taking the inversion of the fundamental or center frequency.

C is the speed of light in vacuum

RDP is the relative dielectric permittivity of the media.

To understand a little bit better the concept, it is marked with “Hr” for horizontal resolution.

$$H_r = \frac{C}{4.f.\sqrt{RDP}} + \frac{D}{\sqrt{RDP+1}} \qquad (5.5)$$

Where:

H_r is the horizontal resolution

C is the speed of light in vacuum

f is the center frequency of the antenna

RDP is the relative dielectric permittivity

D is the depth to the plane where the two objects are located.

For This Thesis we have used the following parameters as the testing value.

Center frequency = 2GHz

RDP = 1.4

D = 100cm

$V_r = \frac{T_{pulse}.C}{2\sqrt{RDP}} \quad = \frac{.5x10^{-9} * 3 * 10^{8}}{2\sqrt{1.4}}$ = 0.063m

$$H_r = \frac{C}{4.f.\sqrt{RDP}} + \frac{D}{\sqrt{RDP+1}} = \frac{3*10^8}{4*2*10^9\sqrt{1.4}} + \frac{1}{\sqrt{1.4+1}} = 0.0317+0.645 = 0.677\text{m}$$

Both vertical and horizontal resolution are illustrated in the Figure 5.5

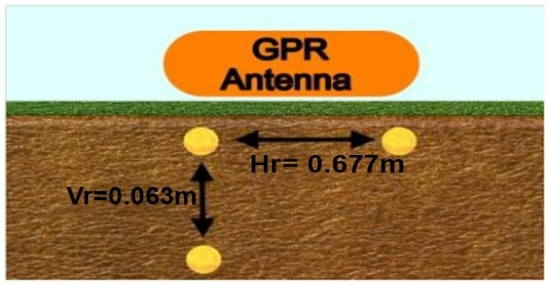

Figure5. 8.Vertical and Horizontal resolution diagram, the golden dots are the targets.

5.3 Scattering-Centre Extraction Algorithm

Scattering centre extraction algorithm include : Model-order (p) estimation, poles (z_k) determination and amplitude coefficients (a_k) estimation .Thus, the high level view of this step is shown in the block diagram of Fig 5.9

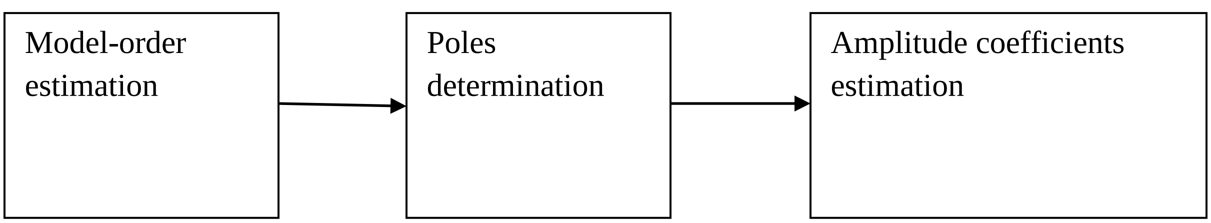

Figure5. 9. Main Steps in Scattering Centre Extraction Algorithm

5.3.1 Model Order Estimation/ Scattering Centre Model Estimation Technique

In this thesis singular value decomposition technique is selected to estimate the model order of exponentially damped radar return signal by exploiting the multiplicity of the eigen-values that are related to the noise.

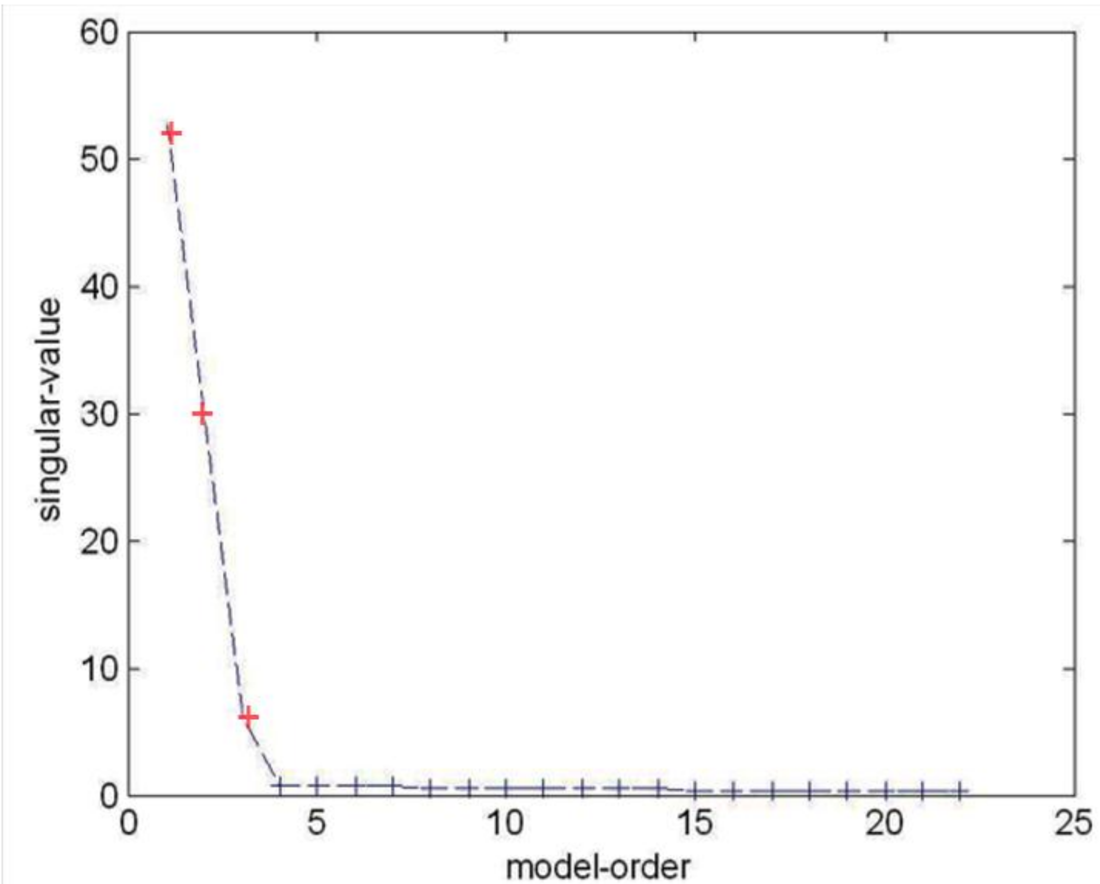

Figure5. 10.Model-order estimation - M = 3, N = 64, L = 22, SNR = 30 dB

For SNR = 30 dB, the transition between groups of singular-values suggests that the model-order is M = 3.

5.3.2 Poles Determination

In this design matrix pencil scattering center extraction algorithms were used to determine the signal pole which is used to estimate the number of scattering center of the target.

5.3.3 Amplitude coefficients estimation

This sub-step includes the investigation of estimates of the exponential amplitude from linear equation.

where is the Moore-penrose pseudoinverse.

Next, the corresponding amplitude coefficients for the L pole estimates are determined from

$$\begin{bmatrix} 1 & 1 & \cdots & \cdots & 1 \\ \hat{p}_1 & \hat{p}_2 & \cdots & \cdots & \hat{p}_L \\ \hat{p}_1^2 & \hat{p}_2^2 & \cdots & \cdots & \hat{p}_L^2 \\ \vdots & \vdots & \cdots & \cdots & \vdots \\ \hat{p}_1^{N-1} & \hat{p}_2^{N-1} & \cdots & \cdots & \hat{p}_L^{N-1} \end{bmatrix} \begin{bmatrix} \hat{\alpha}_1 \\ \hat{\alpha}_2 \\ \hat{\alpha}_3 \\ \vdots \\ \hat{\alpha}_L \end{bmatrix} = \begin{bmatrix} \hat{x}[0] \\ \hat{x}[1] \\ \hat{x}[2] \\ \vdots \\ \hat{x}[N-1] \end{bmatrix} \tag{5.6}$$

or

$$\hat{A}_L \hat{\alpha} = \hat{x} \tag{5.7}$$

Once the L poles and corresponding amplitude coefficients are determined, the extraneous L-p must be separated from the actual p poles and new amplitude coefficients found for the remaining poles.

5.4 Matching Algorithm Using Cluster Approach In Z Plane

Matching Algorithm Using Cluster Approach in z-plane involves three phases; Preprocessing, Feature extraction and Clustering phase. Thus, the high level view of this step is shown in the block diagram of Fig 5.8

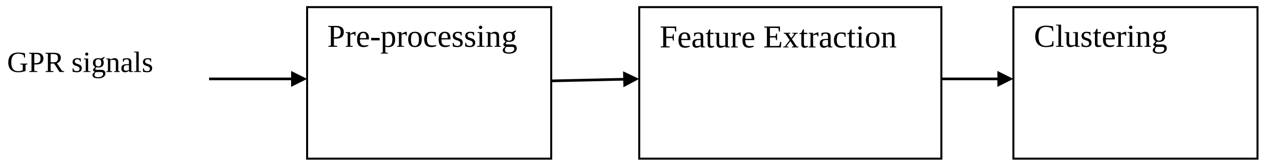

Figure 5. 11. Matching Algorithm Using Cluster Approach in z-Plane system diagram

5.4.1 Pre-Processing Phase

In the pre-processing phase, data are prepared for feature-selection .There are two main steps undertaken in this preprocessing stage:

i. Exponentially damped signal's pole determination

ii. Selecting the true pole which represents the interested scatteter.

Figure 5.8 represents the system diagram leading to the determination and selection of the poles using both the test-signal and the templates in library.

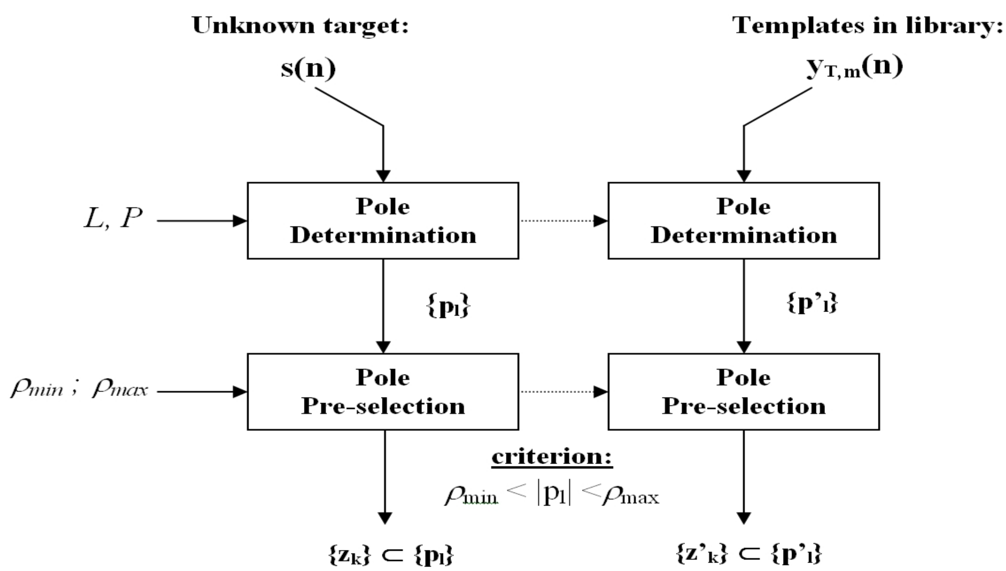

Figure 5. 12. MAUCAZ system diagram - pre-processing stage

5.4.2 Pole determination

Pole of exponentially damped signals can be determined in equation (5.8) as below:
The pole estimates can be obtained from solving for the zeros in the LP polynomial.

$$1+a_1 z^{-1} + a_2 z^{-2} + \cdots + a_M z^{-M} = 1 + \sum_{k=1}^{M} a_k z^{-k} \qquad (5.8)$$

Where

the a_k's are the LP coefficients of the vector **a** in equation (6.8).

5.4.3 Feature Extraction

It consists of extracting from the signal the features that reveal the similarities between the targets compared. They include the way to measure the similarity between patterns of poles, the features to use for the comparison, the differentiation between true poles and extraneous poles, whether the latter are due to the noise, to the technique, or even to extra scatterers on the target.
Feature extraction involves two stages; pole similarity and pole pattern stages. Thus, the high level view of this step is shown in the block diagram of Fig 5.2

Pole Similarity

The main feature of poles of signals Phase angle and Magnitude are extracted to compare the similarity of the poles.

For two aligned patterns, the probability, p(Θ), that two poles are related to scatterers at the same range is an even function of the difference between angles, $\Theta = \theta'm - \theta k$. It has a maximum for $\Theta = 0$, a minimum for $\Theta = \pm\pi$, and, for a given value of Θ, it increases with the variance of the noise.

It can be assumed that the probability, p($\Delta\rho$), that two poles are related to scatterers with geometries leading to similar damping factors is an even function of the difference between their magnitudes, Δρ = ρ′ m−ρk with a maximum for Δρ = 0. Therefore, providing this parameter is accurately estimated, it could be used for classification.

We have considered the true and template signals as $z_k = p_k e^{i\theta_k}$ and $z'_m = p'_m e^{i\theta'_m}$.
we are going to calculate the pole signal phase angle difference as:

$$\Theta = \theta_k - \theta'_m \qquad (5.9)$$

for $\Theta = 0$ and $\Theta = \pm\pi$
And we are going to calculate the pole signals magnitude as below:

$$\Delta p = p_k - p'_m \qquad (5.10)$$

$$\Delta p = 0$$

Pole Pattern

Euclidian distance is used to evaluate the degree of similarity between two sets of K poles [51]. Euclidian distance:

$$d_{Eu} = \left(\sum_{i=1}^{p} d_i^2\right)^{\frac{1}{2}} \qquad (5.11)$$

Gives greater emphasis to larger values of the inter-pole distances.
Where d_i is the inter-pole distance corresponding to a cluster C_i.

Cluster Selection

Figure 5.12 illustrates the clustering approach using a combination of three pairs of poles obtained for M = 5 and M′ = 6. The poles are represented by different markers: (×) for the test-pattern and (+) for the template-pattern. This combination of three dipoles is only 1 out of the 1200 that the 30 possible clusters authorize.

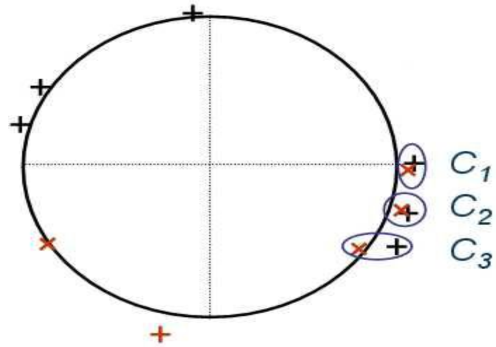

Figure 5. 13.Concept of pole clustering for K = 3, M = 5 and M′ = 6

CHAPTER SIX

RESULTS AND DISCUSSIONS

The design described in chapter six is implemented using Mat-lab software. Therefore, the results and analysis of each step towards target identification and classification is presented in this chapter.

6.1 Model Order determination

In this thesis singular value decomposition is used to estimate the number of scatterer of the target. In the Fig7.1, the model order for sand soil without presence of target is two as the main scatterers are outer surface of the land and the inner part of the soil.

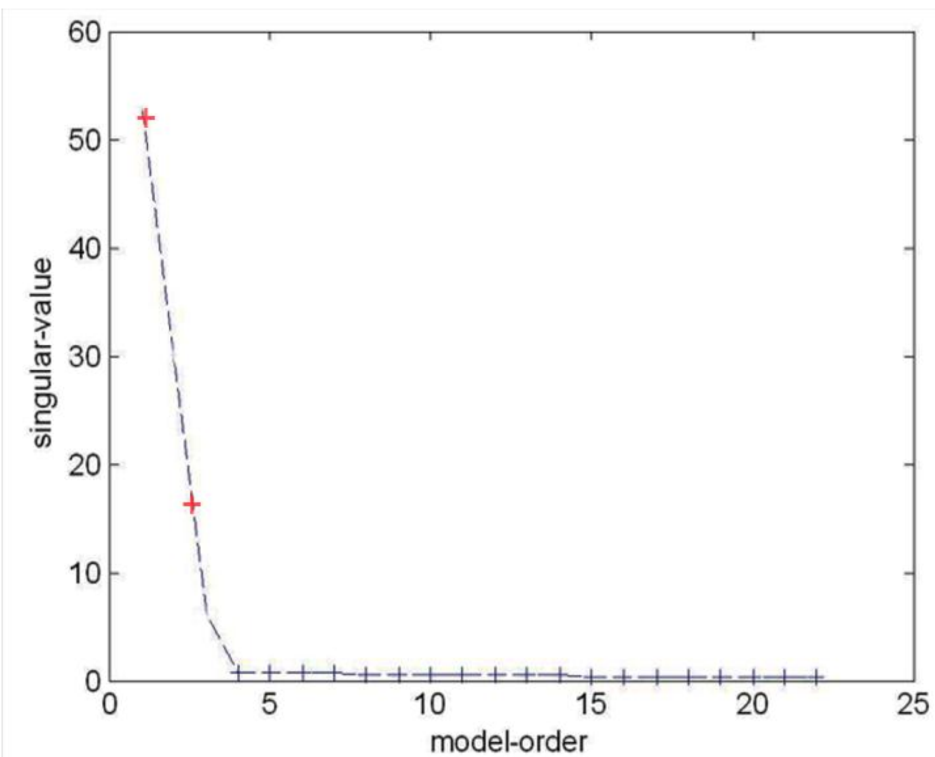

Figure 6. 1.Model-order estimation - M = 2, N = 64, L = 22, SNR = 30 dB

For SNR = 30 dB, the transition between groups of singular-values suggests that the model-order is M = 2.

The number of scatterers for PMN2 Landmine before buried is four as the main reflectors are Case material, internal structure, edge and the starter.

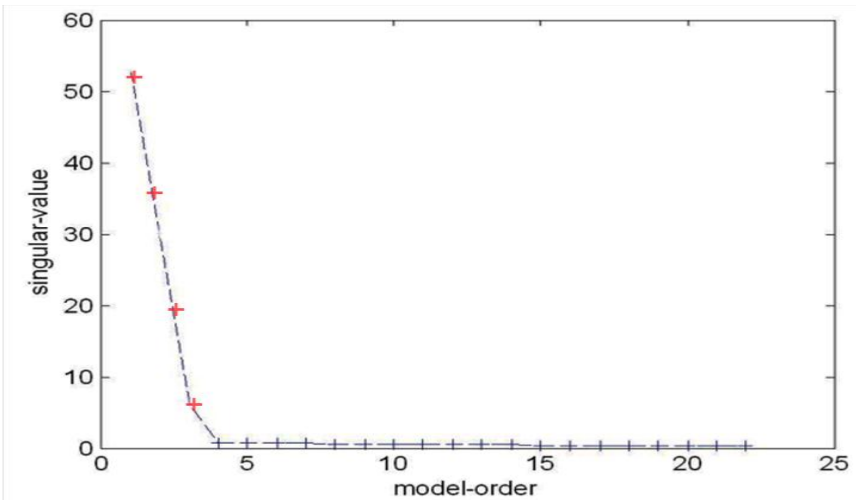

Figure 6. 2.Model-order estimation - M = 4, N = 64, L = 22, SNR = 30 dB

For SNR = 30 dB, the transition between groups of singular-values suggests that the model-order is M = 4.

The number of scatterers for PMN2 Landmine before buried is four as the main reflectors are Case material, internal structure, edge and the starter.

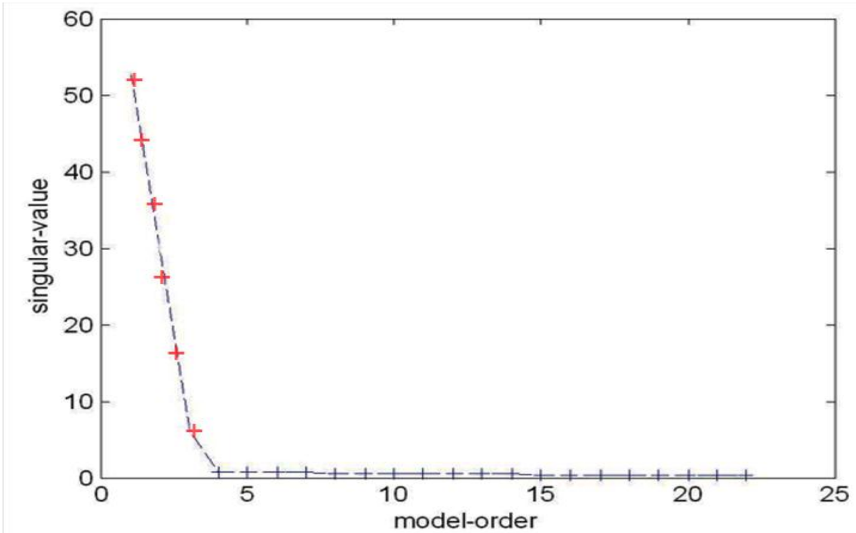

Figure 6. 3.Model-order estimation - M = 6, N = 64, L = 22, SNR = 30 dB

For SNR = 30 dB, the transition between groups of singular-values suggests that the model-order is M = 6.

6.2 Pole extraction and determination

After model order or scattering center was identified, Matrix pencil super resolution algorithm is used to extract the complex signal or poles for each scattering centers.

The estimation of the model parameters of the backscattered GPR echoes corresponding to the sandy soil without the mine presence extracted as the complex conjugate poles $s_1 = -0.04 + j0.22$ *and* $s_2 = -0.04 - j0.22$ and the corresponding amplitudes are $C_1 = 2000 + j3$ and $C_2 = 2000 - j3$. The order of the model is M = 2. At this stage we assumed that the signal is not contaminated by additive zero-mean white Gaussian noise .By applying Matlab we can obtain the following result in figure below.

The two signal poles that fall inside the unit circle are clearly visible, and close to the the unit circle.

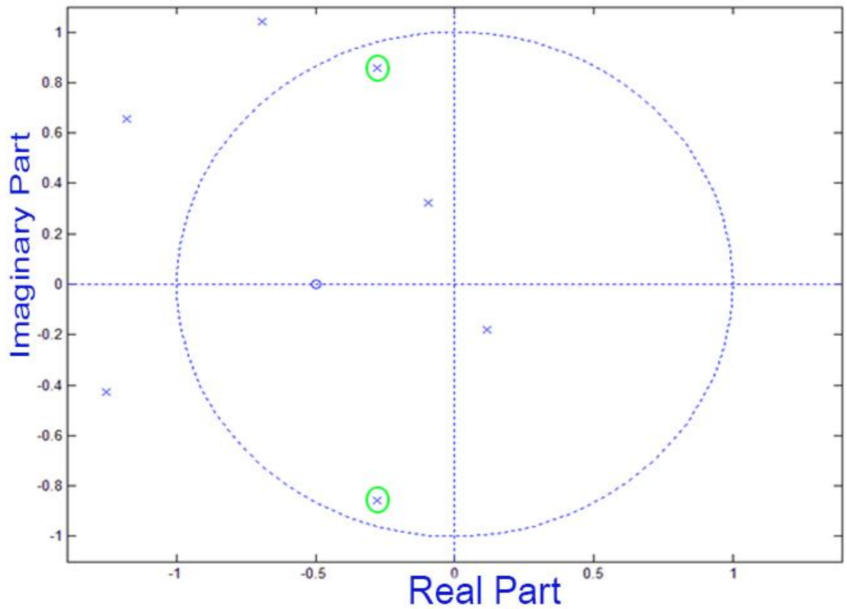

Figure 6. 4.The signal poles are inside the unit circle and close to the unit circle.

The estimation of the model parameters of the backscattered GPR echoes corresponding to the PMN2 mine which is not buried underground, extracted as the complex conjugate poles $s_3 = -0.02 + j0.2$, $s_4 = -0.02 - j0.2$, $s_5 = -0.008 + j0.1$ *and* $s_6 = -0.008 - j0.1$ and the corresponding amplitudes are $C_3 = 2000 + j3$, $C_4 = 2000 - j3$, $C_5 = 100 + j3000$ *and* $C_6 = 100 - j3000$. The order of the model is M = 4. Again we assumed that the signal is not contaminated by additive zero-mean white Gaussian noise .

The zeros of the prediction error filter polynomial B(z) computed for the simulated signal using the Matrix Pencil algorithm and the information-theoretic criterion for the model selection are shown in Figure 6.5. The four signal zeros that fall inside the unit circle are clearly visible, and close to the unit circle are the true poles.

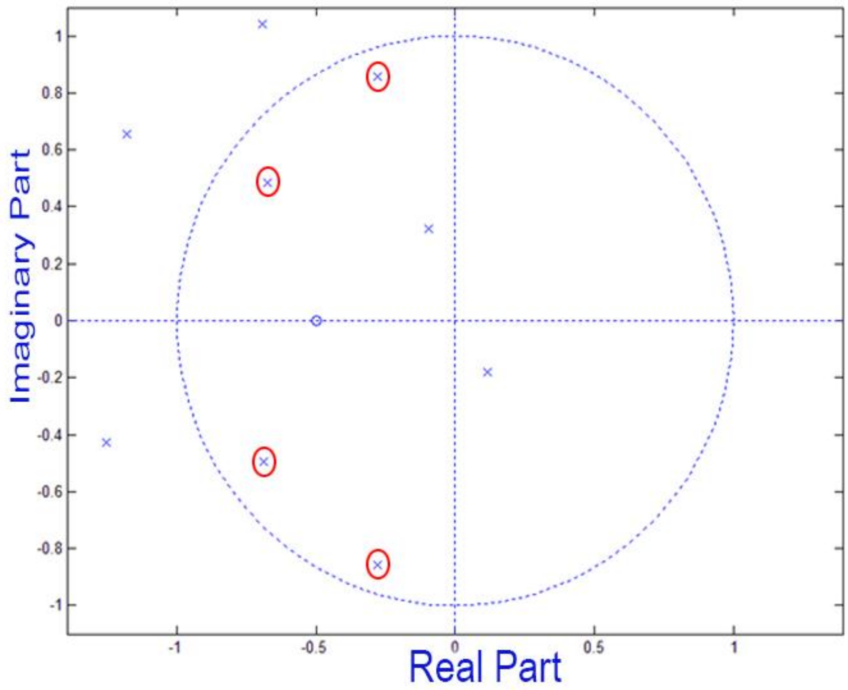

Figure 6. 5.The signal poles are close to the unit circle.

Know let's consider that the PMN2 Landmine was buried under the dry sandy soil at 100cm deep and The complex conjugate poles of this signal are $s_1 = -0.04 + j0.22$, $s_2 = -0.04 - j0.22$, $s_3 = -0.02 + j0.2$, $s_4 = -0.02 - j0.2$, $s_5 = -0.008 + j0.1$ *and* $s_6 = -0.008 - j0.1$ and the corresponding amplitudes are $C_1 = 2000 + j3$, $C_2 = 2000 - j3$, $C_3 = 2000 + j3$, $C_4 = 2000 - j3$, $C_5 = 100 + j3000$ *and* $C_6 = 100 - j3000$. The order of the model is M = 6. The signal is contaminated by additive zero-mean white Gaussian noise with variance $2\delta^2$. Peak signal-to-noise ratio (SNR) used in this thesis is set to 15 dB. This simulated signal contaminated by noise is shown in Figure 6.6

The six signal zeros that fall inside the unit circle are clearly visible, whereas the extraneous zeros are outside and within the unit circle, but not close to unit circle.

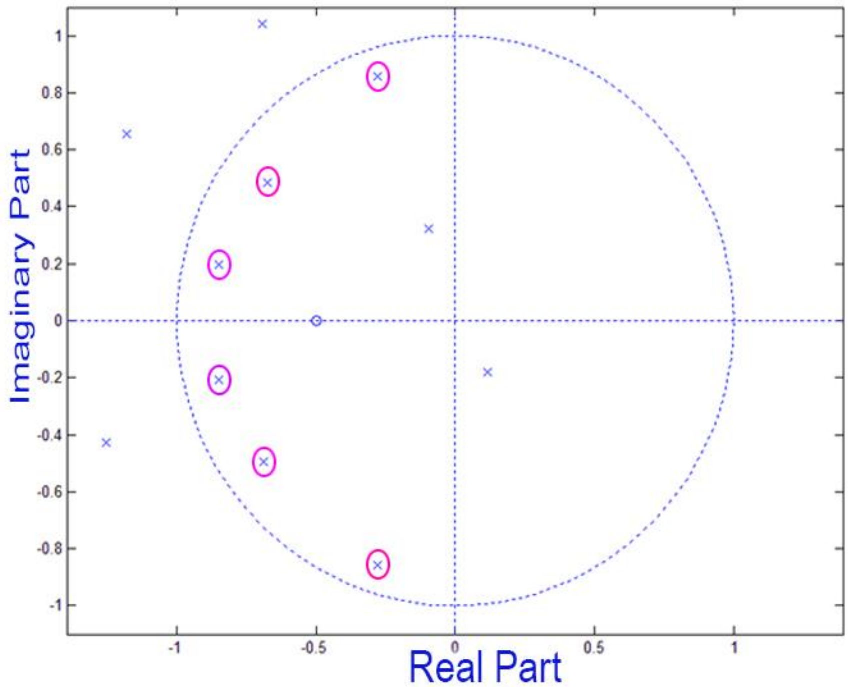

Figure 6. 6.True poles are outside the unit circle, extraneous zeros falls within the unit circle.

6.3 Clustering and classifying targets in Z plane

Figure 6.7 :Illustrates the clustering approach using a combination of three pairs of poles obtained for M =6 and M'= 2.The poles are represented by different markers : black (x) for test pattern of dry sand soil, Green for test pattern of wet sand soil (**x**) ,Blue (**x**) test pattern of sand soil with large grain and Red (x) for the template pattern.

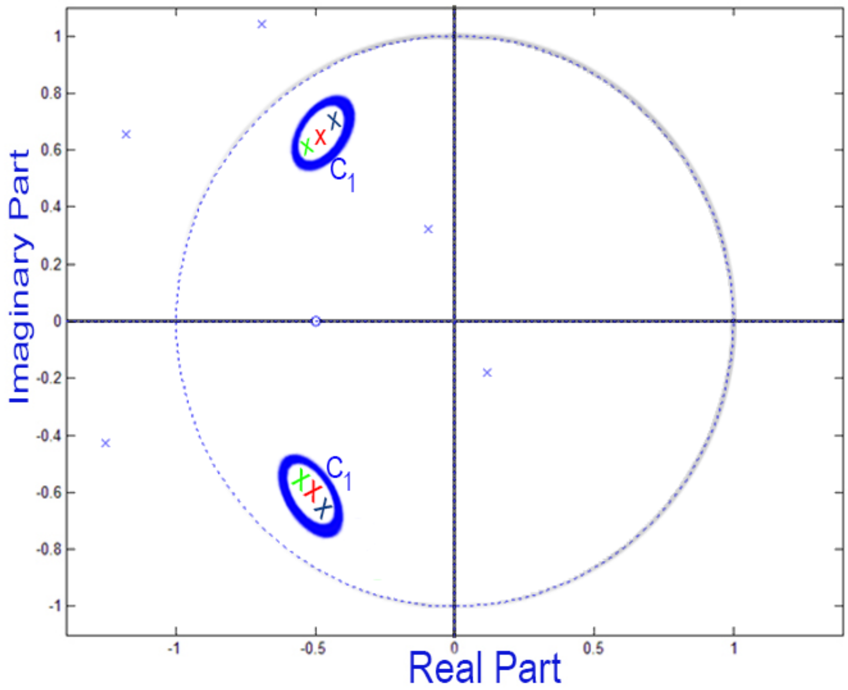

Figure 6. 7.concept of pole clustering for k=3,M=6 and M'= 2

Figure 6.8 :Illustrates the clustering approach using a combination of three pairs of poles obtained for M =18 and M'= 6.The poles are represented by different markers : black (x) for test pattern of dry sand soil, Green for test pattern of wet sand soil (**x**) ,Blue (**x**) test pattern of sand soil with large grain and Red (x) for the template pattern.

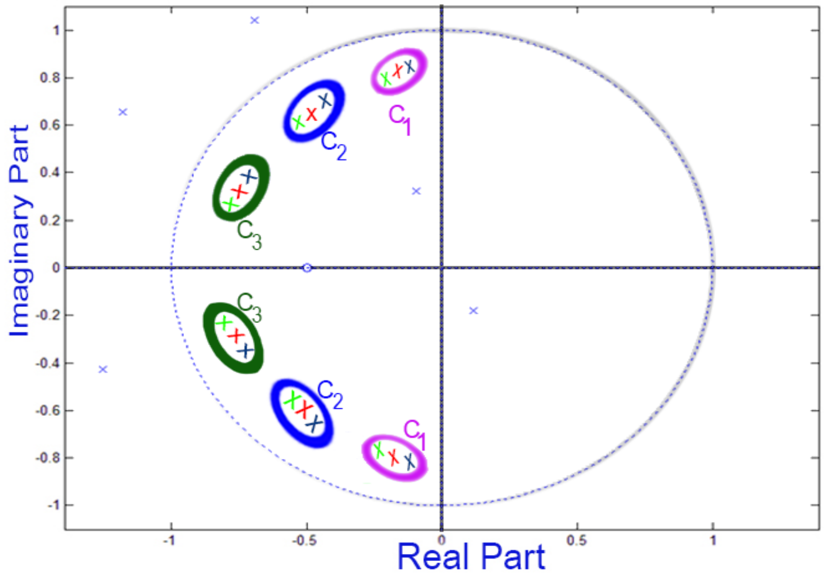

Figure 6. 8. Concept of pole clustering for k=3,M=18 and M'= 6

CHAPTER SEVEN

CONCUSSION AND RECOMMENDATIONS

7.1 Concussion

Developments in Scattering center extraction and MAUCAZ analysis for underground buried targets are an ongoing research area. Most of the works so far have been based on the classification of the underground buried target by using Metal detector and KT algorithm. And detection of nonmetallic object is very difficult with metallic detection method.

Though there is certain algorithm that used to extract the features of subsurface object, as shown in different research, as shown in this work, there were little considerations. Furthermore, this thesis also gave an insight to the necessity of MAUCAZ analysis to classify targets by their poles pattern in z-plane.

Therefore, the Scattering center extraction and MAUCAZ analysis of GPR signals using Matrix Pencil produced promising results. Given, a good preprocessing and feature extraction steps, the Scattering Center extraction and MAUCAZ algorithm is the efficient and robust technique.

By using the model parameters directly expressed in the z-plane, the classifier MAUCAZ is less sensitive to errors on the parameter-estimates than other techniques. This can be explained by the fact that the errors on the pole magnitude have a small influence on the function chosen to measure the distance between patterns.

The combined approach of Scattering center extraction and MAUCAZ presented a higher prediction accuracy compared to the other approach in used previously.

7.2 Recommendations

This work introduced the idea of combining scattering center and MAUCAZ algorithm to detect and classify underground buried targets, either metallic or nonmetallic. But detail research work is required to detect and classify all solid and liquid material at maximum depth.

Furthermore, this study was based on limited data and material for experiment and testing. As a result, the detection and classification was based only on the shallow depth and PMN2 landmine. But for accurate detection, the method should incorporate in database the pole pattern for each material from detail investigation of its laboratory test with different host medium and depth. In addition, the selection of supper resolution algorithm and professional software with the GPR is essential for more reliable detection and classification.

REFERENCE

[1]. Jacqueline MacDonald, J.R. Lockwood, John McFee, Thomas Altshuler, Thomas Broach, Lawrence Carin, Russell Harmon, Carey Rappaport, Waymond Scott,and Richard Weaver, “Alternatives for landmine detection,” RAND Science and Technology policy Institute, 2003.

[2]. Xiaoyin Xu, Eric L. Miller, Carey M. Rappaport, and Gary D. Sower, “Statistical method to detect subsurface objects using array ground-penetrating radar data,” IEEE Transactions on Geoscience and Remote Sensing, vol. 40, no. 4, pp. 963– 976, April 2002.

[3], W. Stern, ”Uber Grundlagen, Methodik und bisherige Ergebnisse elektrodynamischer Dickenmessung von Gletschereis,” Z. Gletscherkunde, vol.15, pp. 24-42, 1930.

[4]. R. M. Morey, ”Continuous subsurface profiling by impulse radar,” Proceedings of the Engineering Foundation Conference on Subsurface Exploration for Underground Excavation and Heavy Construction, pp. 213-232, Aug. 1974.

[5]. J.MacDonald, J. Lockwood, J. McFee,T.Altshuler,and T. Broach ," Alternatives for landmine detection"RAND,2003

[6]. David J. Daniels, Ground Penetrating Radar, The Institution of Electrical Engineers, UK, second edition, 2004.

[7]. Harry M. Jol, Ground Penetration Radar Theory and Application, vol. 1, Elsevier B. V., first edition, 2009.

[8]. David J. Daniels, Paul Curtis, and Oliver Lockwood, “Classification of landmines using gpr,” IEEE Proceedings of International Radar Conference, RADAR ’08., pp. 1–6, May 2008.

[9]. Motoyuki Sato Tohoku University, Sendai 980-8576, Japan sato@cneas.tohoku.ac.jp

[10]. M. Metwaly.National Research Institute of Astronomy and Geophysics, Cairo, Egypt currently at: Graduate School of Engineering, the University of Tokyo, Japan

[11]. ZHENHUA MA Dr. Dominic K.C. Ho, Thesis Supervisor DECEMBER 2007

[12]. L.C. Potter and R.L. Moses, Attributed scattering centers for SAR ATR, Image process., IEEE Trans., 6 (1), pp79-91, January 1997.

13. ISSN 2072-4292 www.mdpi.com/journal/remotesensing , Remote Sens. 2014, 6, 9729-9748; doi: 10.3390/ rs6109729 .

[14]. Yingbo Hua. IEEE Transaction on acoustic speech and signal processing vol.38 No 5 May.1990

.

[15]. Belli, K.M., Ground Penetrating Radar Bridge Deck Investigations Using Computational Modeling, in College of Engineering, Department of Mechanical and Industrial Engineering. 2008, Northeastern University: Boston. p. 235.

[16]. Geophysical Survey Systems, I., GSSI Handbook for RADAR Inspection of Concrete #MN72-367 Rev D. 2006: New Hampshire.p. 38.

[17]. Conyers, L.B., Ground-Penetrating Radar for Archaeology. 2004,Walnut Creek, CA ; Oxford: AltaMira Press.

[18]. Grealy, M., Resolution of Ground-Penetrating Radar Reflections at Differing Frequencies. Archaeological Prospection, 2006. 13(2): p. 142-146.

[19]. Neubauer, W., et al., Georadar in the Roman Civil Town Carnuntum, Austria: An Approach for Archaeological Interpretation of GPR Data. Archaeological Prospection, 2002. **9**(3): p. 135-156.

[20]. Harry M. Jol, Ground Penetration Radar Theory and Application, vol. 1, Elsevier B. V., first edition, 2009.

[21]. Institute of Environmental Physics Heidelberg University Rebecca Ludwig, Holger Gerhards, Patrick Klenk Ute Wollschl□ager, Jens Buchner Version: January 2011

[22] Y.Hua and T.K Sarkar. Matrix Pencil method for estimating parameters of exponentially damped/undamped sinusoids in noise.Acoustics,Speech,and Signal Processing ,IEEE Trans.,38 (23):814-824,1990.

[24] Y.Hua and T.K Sarkar.On SVD for estimating generalised eeigenvalues of singular matrix pencil in noise.Circuits and Systems,1991.,IEEE Internaltional ymposium on ,5:2780-2783,1991.

[25] R.Carriere and R.L Moses.Autoregressivemoving average modeling of radar target signature.In Radar conference 1988,IEEE proc.,pages 225-229.1988.

[26]. The Challenges of Clustering High Dimensional Data Michael Steinbach, Levent Ertöz, and Vipin Kumar

[27].Anil K. Jain and Richard C. Dubes, Algorithms for Clustering Data, Prentice Hall (1988).

[28]. L. Kaufman and P. J. Rousseeuw, Finding Groups in Data: an Introduction to Cluster Analysis, John Wiley and Sons (1990).